polymers

MDPI

*Review*

# Recent Advances in Chitin and Chitosan/Graphene-Based Bio-Nanocomposites for Energetic Applications

**Rabia Ikram [1,*], Badrul Mohamed Jan [1,*], Muhammad Abdul Qadir [2], Akhmal Sidek [3], Minas M. Stylianakis [4] and George Kenanakis [4,*]**

1 Department of Chemical Engineering, University of Malaya, Kuala Lumpur 50603, Malaysia
2 Institute of Chemistry, University of the Punjab, Lahore 54590, Pakistan; mabdulqadir@gmail.com
3 Petroleum Engineering Department, School of Chemical and Energy Engineering, Faculty of Engineering, Universiti Teknologi Malaysia, Johor Bahru 81310, Malaysia; akhmalsidek@utm.my
4 Institute of Electronic Structure and Laser, Foundation for Research and Technology-Hellas, N. Plastira 100, Vasilika Vouton, GR-700 13 Heraklion, Greece; stylianakis@iesl.forth.gr
* Correspondence: raab@um.edu.my (R.I.); badrules@um.edu.my (B.M.J.); gkenanak@iesl.forth.gr (G.K.)

**Abstract:** Herein, we report recent developments in order to explore chitin and chitosan derivatives for energy-related applications. This review summarizes an introduction to common polysaccharides such as cellulose, chitin or chitosan, and their connection with carbon nanomaterials (CNMs), such as bio-nanocomposites. Furthermore, we present their structural analysis followed by the fabrication of graphene-based nanocomposites. In addition, we demonstrate the role of these chitin- and chitosan-derived nanocomposites for energetic applications, including biosensors, batteries, fuel cells, supercapacitors and solar cell systems. Finally, current limitations and future application perspectives are entailed as well. This study establishes the impact of chitin- and chitosan-generated nanomaterials for potential, unexplored industrial applications.

**Keywords:** polymers; graphene oxide; bio-nanocomposites; chitosan; energy



**Citation:** Ikram, R.; Mohamed Jan, B.; Abdul Qadir, M.; Sidek, A.; Stylianakis, M.M.; Kenanakis, G. Recent Advances in Chitin and Chitosan/Graphene-Based Bio-Nanocomposites for Energetic Applications. *Polymers* **2021**, *13*, 3266. https://doi.org/10.3390/polym13193266

Academic Editors: Keiko Shirai, Maribel Plascencia-Jatomea and Neith Aracely Pacheco López

Received: 7 September 2021
Accepted: 23 September 2021
Published: 25 September 2021



## 1. Introduction

In recent decades, nanotechnology advancements have led towards the progressive recycling of natural polymers into a variety of structurally enhanced nanomaterials [1,2]. This has been proven by the synthesis of polymer-based carbon nanomaterials (CNMs) [3]. The implication of CNMs has been established through various fields, such as biological activities [4], drug delivery [5], tissue engineering [6], environmental [7] or energetic applications [8]. Their unique properties have allowed them to be used in several electronic devices [9]. It has been observed that dipole–dipole interactions between molecules and powerful van der Waals forces have produced aggregation among CNMs [10]. Fortunately, the consequences of this limitation, such as the modification of electrical, chemical and mechanical properties, have been modified through functionalization [11]. Graphene is an excellent example of a CNM due to its remarkable attributes, including a large surface area, low weight and excellent thermal as well as mechanical properties [12,13].

Polysaccharides are natural polymeric biomaterials that have been widely used in biotechnological fields due to their availability, biocompatibility and biodegradability [14,15]. Common examples of polysaccharides are starch, cellulose, chitin and chitosan [16]. They can also be modified either chemically or enzymatically for any specific end use. Recently, chitin and chitosan have been used in various applications, including food and nutrition, pharmaceuticals, and biotechnology [17,18]. Owing to its biocompatibility, chitosan has also been deemed a suitable material for wastewater treatment, as well as for medicinal and electrochemical applications [19,20]. As nanotechnology advances, the fabrication of chitosan nanocomposites with organic and inorganic nanofillers has significantly improved the material's mechanical, chemical and barrier properties [21]. These remarkable results

are squandered as there are no works in the literature that study systematic nanostructures, novel bio-nanocomposite possibilities and their associated fabrication processes, which are needed. As a result, this study aims to bridge that gap by presenting future trends as well as challenges associated with chitin and chitosan as a matrix for bio-nanocomposites.

Over the past few years, chitin- and chitosan-derived nanocomposites have shown a tendency towards a wide range of applications. Recently, chitin- and chitosan-based nanomaterials and their remarkable role as dye adsorbents [22], drug delivery vehicles to combat COVID-19 [23], food packaging [24], membranes [25], wound dressings [26] and for biomedical and environmental applications [27,28] have been presented.

To the best of our knowledge, there have been very limited studies which have summarized, in particular, chitin- and chitosan-based nanocomposites for energy-related applications. This work is briefly organized into the background of graphene and graphene oxide (GO) properties as well as the structural properties of chitin/chitosan. In addition, common methods for the fabrication of chitin- and chitosan-derived graphene bio-nanocomposites have been discussed. Finally, it reveals vital information of chitin/chitosan bio-nanocomposites for applications in electronic devices and energy systems. To make it more instructive, this study also presents future recommendations and challenges of current times.

## 2. Graphene and Graphene Oxide

Research related to compatible two-dimensional (2D) CNMs, such as graphite and diamonds, has expanded [29]. Graphene, which is derived from graphite, has been used in a variety of applications. Single-layer graphene was explored theoretically by P. R. Wallace in 1947. It was first unambiguously produced and identified in 2004 [30,31]. Many efforts have been made to mass-produce graphene in selected industries, particularly materials science and chemistry [32]. According to recent price checks, allocated budgets for graphene fabrication and the production of its derivatives reached $67 million in 2015, and are estimated to increase to $680 million by 2020 [33]. Graphene is composed of a single layer of hexagonal graphite with $sp^2$-hybridized carbons and sigma connections [34]. Furthermore, delocalized $\pi$-type bonds are formed from the remaining p or $\sigma$ orbitals. It has a two-dimensional structure composed of a layer of carbon atoms that are covalently connected in the form of hexagonal lattices [35]. This is the fundamental structure of many carbon allotropes [36].

Graphene possesses unique properties, such as a 1.42 Å carbon–carbon connection interval, a 3.3 Å thickness, a large surface area, high movement ability and significant optical, mechanical, electrical and thermal properties [37,38]. Meanwhile, GO was produced by the oxidation of graphite, which is composed of graphene and other functional groups, such as –C=O, –OH, –COOH and –COC– [39]. The existence of oxygenated functional groups on the surface of GO has caused it to have higher capacitance than graphene despite having a smaller surface area [40]. Both GO and reduced graphene oxide (rGO) have great potential to be used in energy-related applications due to their high capacitance, impressive efficiency and enhanced properties as compared to graphene [41,42]. A wide range of synthetic methods have been utilized to convert graphene from waste materials, which are presented in Figure 1.

### *Chitin and Chitosan; Structural Analysis*

Chitosan, the world's second most abundant biopolymer [43], is composed of N-acetyl glucosamine and glucosamine residues [44]. It is a valuable polymer as it can be easily obtained from marine wastes, including crustaceans and microorganisms such as fungi [45]. Chitosan can be produced in a variety of molecular weights (MWs) and degrees of de-acetylation (DA). Following the DA process, chitosan has been extracted from the solution in the form of powder, fiber and sponges [46]. The solubility of chitosan has a large influence on the ionic concentration, MW, pH, acid nature, DA and distribution of acetyl groups, as well as the main chain. Chitosan is usually dissolved in weak acids, most

notably 1% of 0.1 M acetic acid [47]. Furthermore, chitosan can be dissolved in water in the presence of glycerol 2-phosphate at a neutral pH [48]. This type of chitosan is appropriate for plant-based applications [49]. A stable solution can be obtained at room temperature. On the other hand, it endorses reversible gel formation above 40 °C. In comparison to chitin, chitosan possesses better complex-forming ability, which has been attributed primarily to the existing free $–NH_2$ groups distributed along its main chain (Figure 2) [50]. Chitosan, a partially deacetylated chitin product, is a copolymer composed of β-(1→4)-2-acetamido-D-glucose and β-(1→4)-2-amino-D-glucose units [51]. In chitosan structure, the R1, R2 and R3 radicals correspond to hydrogen available in plain chitin and chitosan molecules. These surface groups result in the formation of hydroxyl (OH) and amino ($NH_2$) groups. They are accountable for the organic modifications of chitosan, which have the potential to produce polymeric derivatives of these compounds [52].

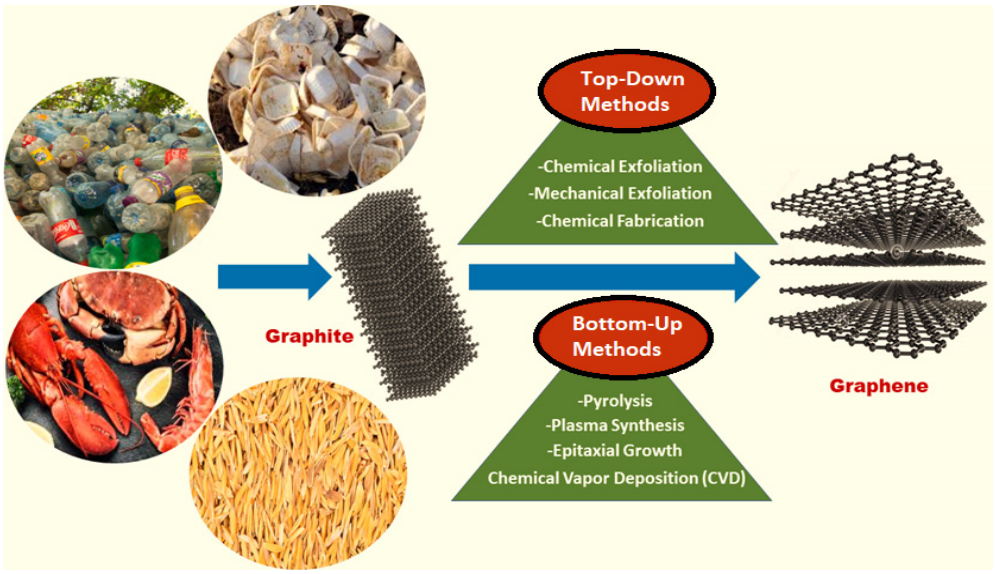


**Figure 1.** Schematic illustration of graphene synthetic routes from waste sources.

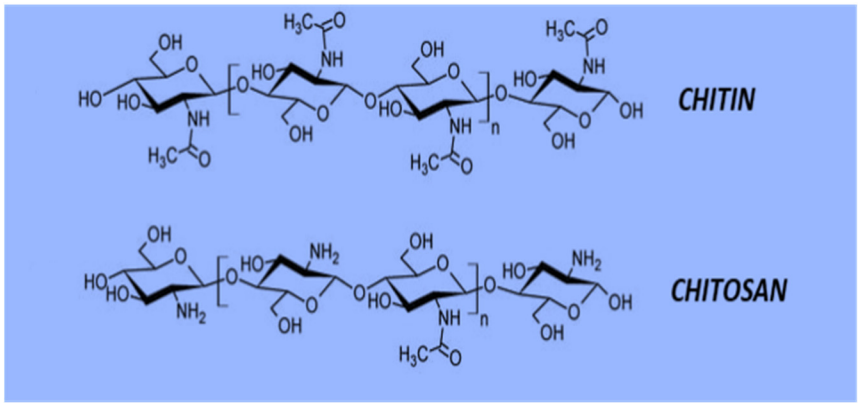


**Figure 2.** Structural analysis of chitin and chitosan. Reproduced with permission from [53].

Crustacean shell wastes are a source of biomass raw material for chitin and chitosan production. They contain chitin, lipids, inorganic salts and proteins, as displayed in Figure 3 [54]. Numerous characterization techniques, such as SEM, FTIR, DSC, TGA, 1H liquid-state NMR, XRD and elemental analysis have been used to investigate morphological, structural, degree of DA, crystallinity and other physicochemical or thermal properties [50,55].

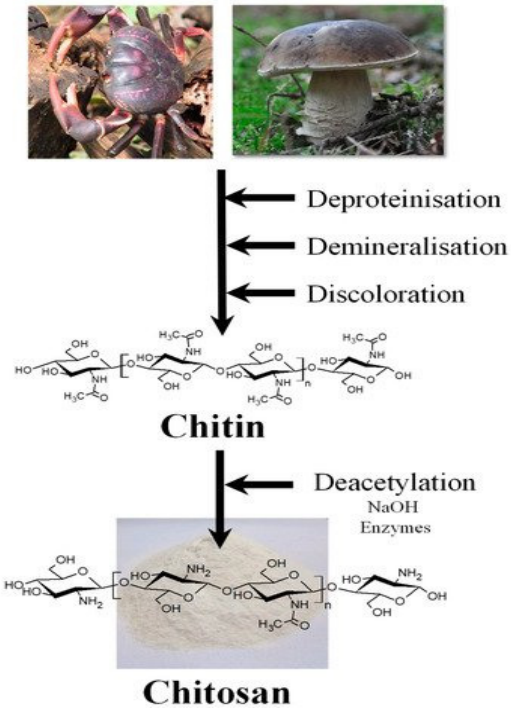


**Figure 3.** Mechanism of crustacean shell waste conversion into chitin and chitosan [53].

## 3. Fabrication of Graphene Nanocomposites

The distribution of materials in polymeric matrices has a significant influence on the mechanical, thermal and electrical properties of nanocomposites, as well as their water vapor permeability [56]. Poor distribution of biopolymer–graphene/GO produces unstable nanocomposites, and jeopardizes their properties. The aggregation of graphene/GO nanoparticles and restacking into biopolymeric materials has been a concerning issue [57]. For example, water-soluble polymers such as poly(vinyl alcohol) and poly(ethylene oxide) have been used in the fabrication of GO nanocomposites [58]. Earlier studies have revealed that graphene/GO fillers were incorporated into polymer matrices through common methods, such as solution intercalation, electrospinning and in situ intercalative polymerization, as shown in Figure 4 [59,60].

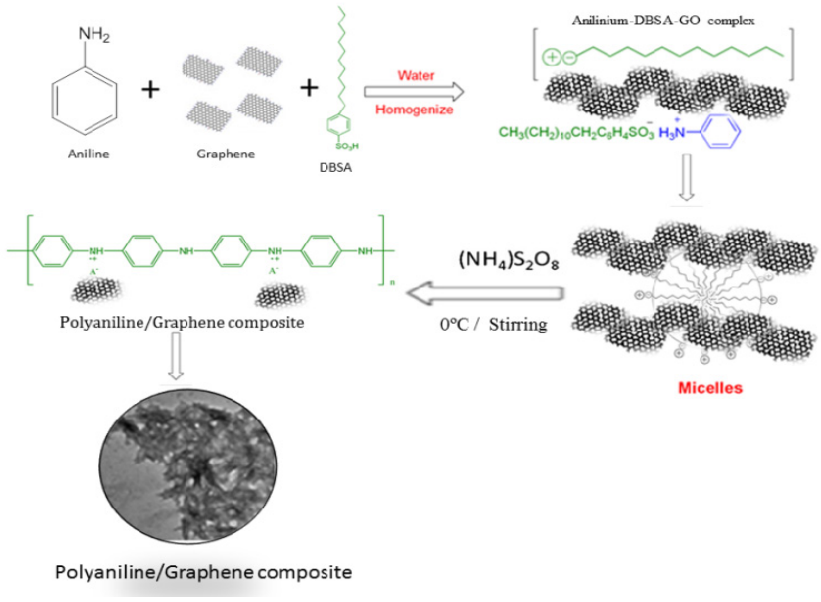


**Figure 4.** Fabrication of a polymer-based (polyaniline) graphene nanocomposite [61].

Most researchers have used a solution intercalation method, in which the chemical structure of a polymer matrix changed as the amount of graphene/GO increased [62]. This was attributed to the occurrence of mild chemical reactions, primarily physical interactions between biopolymers and graphene/GO [60]. Characteristically, this method involves shear mixing of colloidal graphene/GO suspensions with polymers, followed by solvent evaporation. As a result, the adsorbed polymer reassembled, forming a sandwich between the polymer and graphene/GO [63]. Furthermore, polymer–graphene/GO matrices were used in solution-based methods with non-water-soluble polymers via the chemical modification of GO [64]. Poly(methyl methacrylate) and polyurethanes are two examples of non-soluble polymers that have been used in this method [65]. Another interesting method of preparing graphene/GO bio-nanocomposites is in situ polymerization, which uses solvents to lower the dispersions' viscosity [66]. For example, GO has prepared nanocomposites with enhanced properties by intercalative polymerization of poly(methylmethacrylate) [67] and epoxy resins [68]. Furthermore, polyethylene [69] and polypropylene matrix GO nanocomposites [70] have been successfully prepared via in situ polymerization.

Poly(methylmethacrylate) chains were grafted onto GO to make the filler compatible with the polymeric matrix [71]. The melt-blending method has been used to disperse thermally reduced GO into polymers as well as into a renewable polylactide [72]. Satisfactory distribution rates are attainable through this process. However, it increases polymer melt viscosity, which complicates the process. The preparation of polymer composites, such as graphite, into polypropylene has been done by solid-state shear dispersion using a modified twin-screw extruder [73]. Table 1 entails the synthesis of graphene nanocomposites, comprising polymeric and other matrices, for an enormous number of applications.

**Table 1.** Summary of the graphene nanocomposites with inorganic and polymeric materials.

| Counterparts | Manufacturing Methods | Parameters and Conditions | Applications | Ref. |
|---|---|---|---|---|
| **Graphene–Polymer Nanocomposites** | | | | |
| Three-dimensional graphene-based polymer nanocomposite | Three methods were used;<br>• Three-dimensional graphene-based template<br>• Polymer particle/foam template<br>• Organic-molecule-cross-linked graphene | - | • Energy storage and conversion<br>• Electromagnetic interference shielding<br>• Oil/water separation<br>• Sensors | [74] |
| Polyaniline/GO nanocomposite | Electrospinning technique | • Detection limit: 0.01 mg/g | • Determination of nicotine | [75] |
| Polyaniline/GO nanocomposite | Chemical exfoliation | • Detection limit: 0.1 µg/L<br>• Quantification limit: 0.4 µg/L | • As adsorbent in the presence of chelating dithizone ligand to measure cadmium (II) ions in aqueous media | [76] |
| Hydrogels of conjugate polymer polypyrrole (PPy)/rGO composite | - | • Surface area: 21.48 $m^2/g$ | • As heavy metal sensors for simultaneous detection of $Cd^{2+,}$ $Pb^{2+,}$ $Cu^{2+}$ and $Hg^{2+}$ | [77] |
| Polylactic acid (PLA)/GO nanocomposite | Solution blending and coagulation | • PLA/GO 1 wt.% | • Enhanced mechanical properties | [78] |
| Polyurethane–GO nanocomposite | - | • Thermal stability increased to 217 °C<br>• Good electrical conductivity: $1.39 \times 10^{-9}$ $Scm^{-1}$ | • Sensing material for optical fibers | [79] |
| Polyaniline nanofibers/functionalized rGO composite films | Hybrid suspension of GO and in situ polymerized polyaniline nanofibers were filtered, followed by hydrothermal treatment | - | • Composite films were uniform, flexible and stable<br>• High specific capacity: 692 F/g at 1 A/g<br>• As electrodes<br>• High capacitance of 324.4 F/g at 1 A/g<br>• Energy density: 16.3 Wh/kg at power density of 300 W/kg | [80] |
| Bacterial cellulose/graphene/polyaniline nanocomposite | Two-step strategy | • Electrical conductivity: $1.7 \pm 0.1$ S/cm | • Electromagnetic shielding<br>• Flexible electrodes | [81] |

**Table 1.** *Cont.*

| Counterparts | Manufacturing Methods | Parameters and Conditions | Applications | Ref. |
|---|---|---|---|---|
| **Graphene/Activated Carbon Nanocomposites** | | | | |
| AG/PMB/GS/GCE | Ag nanocrystals were electrodeposited on different polymer dyes, poly (methylene blue) or poly (4-(2-Pyridylazo)-Resorcinol) (PAR)-modified graphene carbon spheres (GS) hybrids | • Detection limit: 0.15 μM<br>• Sensitivity: 400 μAm/Mcm$^2$ | • Sensor for $H_2O_2$ detection | [82] |
| rGO/activated carbon nanosheet composite | - | • Specific capacitance of the electrode material by 58.2% | • High-performance electrode material for supercapacitor | [83] |
| Glucose-treated rGO–activated carbon (rGO/AC) composites | Hydrothermal technique | • Detection of glucose in range of 0.002 to 10 mM<br>• Sensitivity: 61.06 μA/mMcm$^2$<br>• Response time: 4 s<br>• Low detection limit: 2 μM | • Biosensor | [84] |
| **Graphene/Metal Oxide Nanocomposites** | | | | |
| HBcAG/gold nanoparticles–rGO–enAu nanocomposite | - | • Lowest detection limit: 3.8 ng/mL at 3 σ/m | • Anti-hepatitis antigen detection | [85] |
| Fe-doped $SnO_2$/rGO nanocomposite | Fe-doped $SnO_2$ was hybridized with different iron concentrations and rGOHydrothermal method | - | • Photocatalysis | [86] |
| ZnO–graphene composite | Hydrothermal method | • Band gap energy: 2.84 eV<br>• Photoluminescence lifetime: 21.60 ns | | [87] |
| $TiO_2$/rGO nanocomposite | - | • Good catalytic activity<br>• Cooking oil converted into biodiesel at a rate of 98% | • Heterogeneous catalyst for transesterification of waste cooking oil into biodiesel | [88] |
| GO–$Cu_2O$ nanocomposite | - | • Agglomerated Cu nanoparticles were distributed uniformly over rGO sheets at 400 °C<br>• Electrical conductivity similar to GO monolayer sheets | • Supercapacitor | [89] |
| 2D $MnO_2$/rGO nanocomposite | Wet chemical method at low temperature | • Discharged specific capacity maintains at 242 mAh/g after 60 cycles at 0.1 C | • Cathode material of lithium-ion batteries (LIBs) | [90] |
| rGO/silver nanowires (AgNWs)/Ga-doped zinc oxide (GZO) composite thin films | - | • Excellent electrical conductivity<br>• Superior stability to a mono/bilayer of electrodes<br>• Resistance increased to less than 5% when exposed to atmosphere for 60 days | • Composite electrode | [91] |
| rGO/CuO nanocomposite | Impregnation of microsized malachite spheres on GO sheets followed by calcination at 300–500 °C for 5 h | • Efficient nanocatalysts compared to CuO nanoparticles | • Catalyst | [92] |
| 3D NiO hollow sphere/rGO composite | Coordinating etching and precipitating process by using $Cu_2O$ nanosphere/GO composite as a template | • Sensitivity: 2.04 mA $mM^{-1}cm^{-2}$<br>• Response time: 5 s<br>• Good stability | • Glucose sensor | [93] |
| $Fe_2O_3$/rGO composite | Hydrothermal method | • Specific discharge battery: 1366 mAh/g at 0.1 A/g (LIBs) and 318.9 F/g at 0.1 A/g | • Electrode material for supercapacitor<br>• Anode material for LIBs | [94] |
| **Graphene/Metal Nanocomposites** | | | | |
| rGO/$Co_9S_8$ composites | - | • High discharge capacity: 551 mAh/g at 0.1 A/g<br>• Good rate capability at 10 A/g | • Advanced sodium-ion battery anode<br>• $Na_3V_2(PO_4)_3$krGO/$Co_9S_8$ full cells | [95] |
| Three-dimensional porous-laser-induced graphene–silver nanocomposite | - | • High uniform electrical conductivity<br>• Low detection limit: 5 μM | • Glucose sensor | [96] |

**Table 1.** *Cont.*

| Counterparts | Manufacturing Methods | Parameters and Conditions | Applications | Ref. |
| --- | --- | --- | --- | --- |
| Nitrogen-doped graphene–copper nanocomposite | | • Electrical resistivity: 0.16 μΩ cm at room temperature<br>• Thermal conductivity: 538 W/mK at 25 °C | • High thermal conductivity | [97] |
| SH-β-CD-rGO/Cu nanospheres nanocomposite | Chemical deposition of Cu nanospheres on SH-β-CD-rGO | • Good sensitivity<br>• Low detection limit: 20 nM | • Used for rapid and sensitive electrochemical method to determine trace 4-NP in water | [98] |

*Chitin and Chitosan Graphene Bio-Nanocomposites*

GO is an oxidized and hydrophilic form of graphene which greatly enhances functionalities of polymeric matrices [99]. Both graphene and GO are commonly utilized as a nanofiller in polymeric nanocomposites. Chemical modification of graphene has resulted in high-performance nanocomposites with enriched characteristics [100]. Several techniques have been employed to evenly disseminate graphene or GO into chitosan matrices by developing physical/chemical linkages [101].

Chitosan is a green, sustainable and low-cost material. Chitosan-derived nanocomposites have captivated the interest of many researchers due to their exceptional chemical and physical properties [102]. Advances in nanotechnology has led to nanoparticles being deposited on the surface of chitosan. Apart from being used as a pure matrix biomaterial, other nanoparticles have been embedded in bulk materials. Due to chitosan's hydroxyl (OH) and amine ($NH_2$) surface groups, it encourages several inter- and intramolecular hydrogen bond formations [103]. It allows the usage of inorganic and organic fillers, which improves functionalization [104].

Some researchers have doped graphene/GO bio-nanocomposites with starch, chitosan, cellulose and poly(hydroxyalkanoates) [105]. New techniques, such as emulsion droplet coalescence, sieving and spray drying have been applied for the fabrication of chitosan-based products, which are primarily used in medical and pharmaceutical applications [106,107]. The development of new nanocomposite materials continues to be hampered for agricultural applications; however, it is feasible if the source material is equally inexpensive and compatible. Nonetheless, due to chitosan's properties, it has been used in the fabrication of suitable nanocomposites [108].

Ionic gelation and spray drying are regarded as the best protocols for large-scale CNM production [109]. The ionic gelation method involves the interaction of positively charged chitosan amino groups with negatively charged tripolyphosphate (TTP). TTP is an anionic crosslinker that forms nanoparticles by interacting with chitosan molecules. It is non-toxic and devoid of any innate biological activity. As a result, it is widely used in the production of CNMs [110]. The resulting nanocomposites have been used for foliar applications.

According to a study on the chitosan–rGO nanocomposite, rGO was incorporated into the chitosan crystalline network to improve the adsorption and dye attraction properties of fabricated nanocomposites [111]. At 6 wt.% of rGO nanocomposite, tensile strength, Young's modulus, elongation at break and conductivity values were increased. However, aggregation occurred at 7 wt.% of rGO, and nanocomposite film conductivity was decreased [112].

Another study on the chitosan-GO nanocomposite reported the existence of a strong interaction between GO and chitosan [113]. An FTIR analysis revealed two peaks, one of which was the amine stretch of chitosan, and the other belonged to the OH group of GO. The fabricated nanocomposites showed properties that were identical to chitosan and GO. Peaks associated with the C=C bonds of GO moved to lower wavenumbers. It occurred due to hydrogen bonding between GO and the chitosan network [114]. In the XRD study, GO was completely exfoliated when the diffraction angles of the chitosan-GO composite were similar to those of the chitosan film. Furthermore, the presence of GO in the composite resulted in lower crystallinity due to a longer combination period [115]. Figure 5 represents the fabrication of the chitosan/GO nanocomposite through ultrasonication for 30 and

120 min, followed by AFM morphological analysis. The cross-linkage between chitosan and GO has been evaluated along with their physical properties [116].

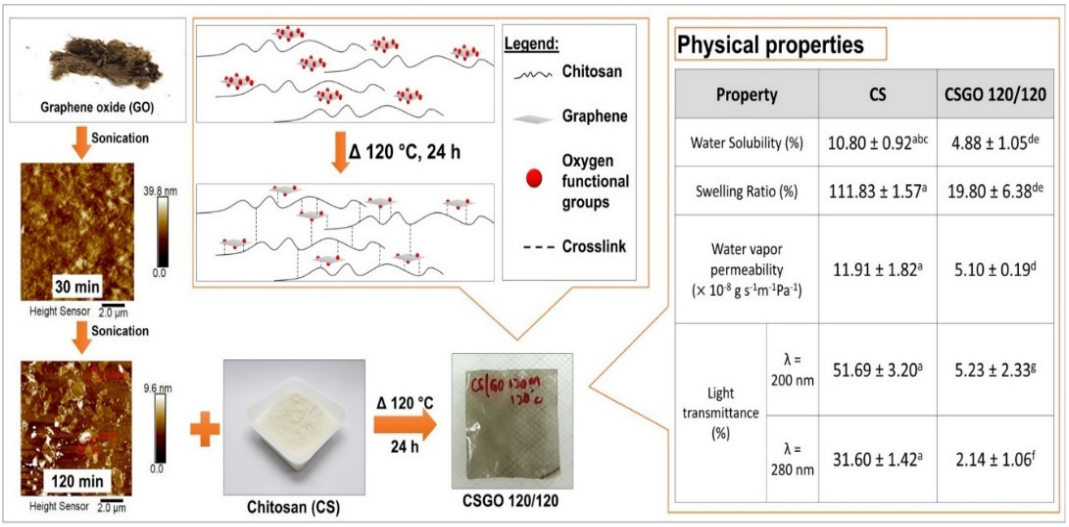


**Figure 5.** Fabrication of chitosan/GO nanocomposite via ultrasonication which controlled the size and thickness of GO nanosheets. The nanocomposite thin film showed a remarkable decline in UV transmittance, a temperature of 120 °C and compacted hydrophilic properties [116].

Cobos et al. prepared free-standing chitosan–GO nanocomposite films [117]. During the process, GO was dispersed homogenously in chitosan due to the amide linkage formation between carboxylic acid groups of GO and amine groups of chitosan. As compared to pure chitosan, the glass transition temperature of the chitosan–graphene nanocomposite was increased from 118 °C to 158 °C [118]. Furthermore, the tensile strength and Young's modulus of synthesized nanocomposite was increased by 2.5 and 4.6 times, respectively [119]. In a very recent study, Zhang et al. have synthesized functionalized GO (fGO), by combining chitosan and ionic liquid, for use as an electrochemical sensor, which is displayed in Figure 6. This novel electrochemical senor has been successfully utilized for amaranth detection in commercial beverages, with excellent results [120].

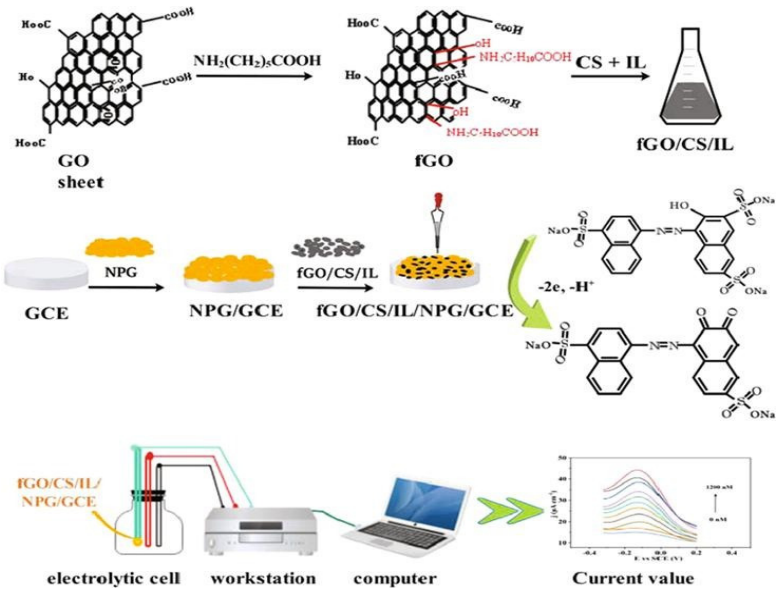


**Figure 6.** Schematic analysis of novel electrochemical sensor prepared by fGO/chitosan/ionic liquid nanocomposite [120].

## 4. Energetic Applications of Chitin and Chitosan

The enhanced properties of polymeric materials with metal oxide nanoparticles into composite electrodes have been optimized through the long, linear backbones of chitin and chitosan for electronic devices [121]. This type of synthesis has been conducted to create a hierarchical assembly which connects nanoscopic metal oxide particles to the macro-scale structure of chitosan through electrochemical deposition [122]. Further studies are focused on the MW of chitin and chitosan, which has effected the capacitive behavior and cyclic stability on electrodeposited thin films [19,123].

Chitin and chitosan have emerged as significant polymers for the production of soft materials. This is due to the combination of physicochemical characteristics of biopolymers that enables the hierarchical assembly of nano-sized components at different length scales [124]. The characteristics of chitin and chitosan are influenced by the amount of glucosamine repeating units, crystallinity and degree of DA [125].

### *4.1. Electrical Devices*

The development of high-performance composite materials has been expedited by incorporating inorganic "nano-fillers" into polymers. Conventionally, the uses of polymer–inorganic nanocomposites include mechanical, optical, catalytic, magnetic, thermal, electrical and electrochemical applications [126,127]. It is highly desired to attain cost-effective and high-tech functionalized electronic devices for commercial uses. Hence, metal-filled polymer composites are seen as a viable option to meet the requirements of future dielectric technologies [128].

Nanoparticles are engineered to sustain high electron mobility in order to achieve fast field responses with extraordinary dielectric constants and minimal losses in high-frequency applications [129]. The engineered bio-nanocomposite dielectrics have higher dielectric constants at elevated frequencies and can process polymers at low temperatures as compared to other conventional materials (Figure 7) [130]. Chitosan is preferred in current research prospects due to its ease of accessibility, low cost, environmental friendliness and outstanding mechanical characteristics [131].

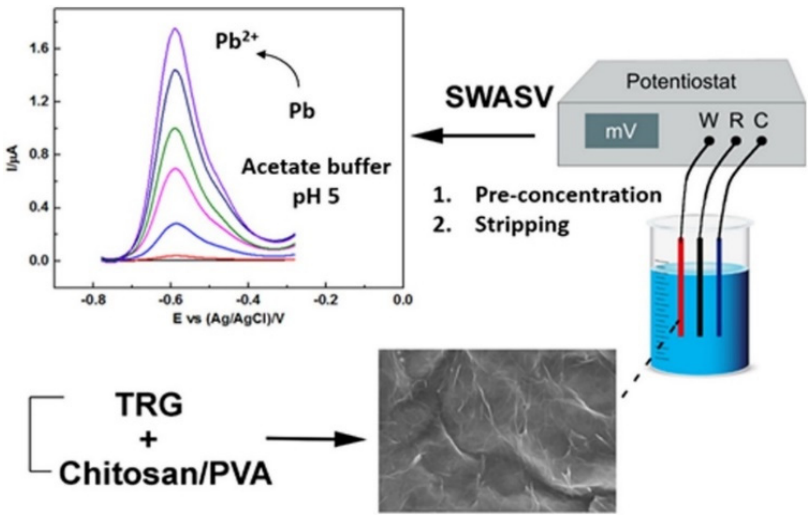


**Figure 7.** Modification of thermally reduced graphene/chitosan/polyvinyl alcohol nanocomposite as an electrode for Pb(II) detection in wastewater [132].

In recent years, CNMs such as carbon nanotubes (CNTs) and graphite have been tremendously used among several electronic devices [133]. Metal oxides, such as ZnO, SiO, NiO and $TiO_2$, are typically doped as inorganic nano-fillers for electrical and electrochemical purposes [134]. The dielectric characteristics of NiO have been utilized in the form of nano-fillers for a handful of studies. NiO is a Mott-Hubbard insulator with an extremely low conductivity at ambient temperatures, and has a cubic lattice parameter of

0.4177 nm [135]. However, when the size is lowered to nanoscale, the conductivity of NiO increases significantly due to hole hopping associated with $Ni^{2+}$ vacancies. By incorporating these fillers into non-conducting polymers, they have transformed into conductive polymers while preserving their polymeric properties [136].

Nasrollahzadeh et al. studied in great depth the possibilities of chitin and chitosan as length-scale interconnects. Among the linear carbon backbone of biopolymers, chitosan has provided a location for nanocomponents/fillers linkage within the range of 100–101 nm [137]. The biopolymer exhibits self-organizing properties contributed from the chitosan's stimuli-responsive film and gel-forming characteristics at microscale levels. Therefore, assembly at greater length scales, i.e., 103 nm, is enabled [138]. Furthermore, localized electrical stimulation promotes the formation of chitin- and chitosan-based films and gels. As a result, both the length scale and nanoscale components of chitosan were linked to electrical equipment. Finally, the metal binding capabilities of chitosan enabled linkages through chelation processes [139]. Kamran et al. have discovered acetic-mediated chitosan-based porous CNMs, which resulted in the capture of $CO_2$. They also demonstrated an enhanced surface area (4168 $m^2$ $g^{-1}$) and highly effective $CO_2$ adsorption performance of fabricated nanomaterials [140]. Currently, there are minimal studies in the literature on the electrochemical behavior and energy production of such novel bio-nanocomposites.

### *4.2. Biosensors*

Recently, there has been remarkable use of cost-effective and economic biosensors in energy-related applications [141]. High-quality immobilization of biological recognition components is required to generate dependable biosensors. Chitosan and its bio-nanocomposites have been introduced as effective immobilization matrix materials. Thus, development of novel devices for early-stage illness diagnosis and biomarker detection were possible through these chitosan-bio-nanocomposites-based biosensors (Figure 8) [142].

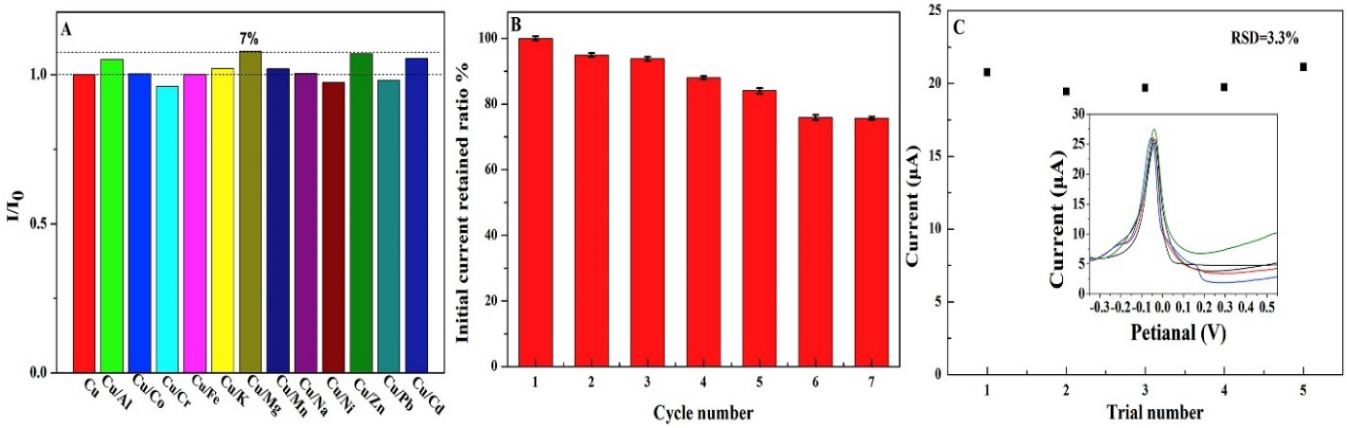


**Figure 8.** (**A**) Selectivity, (**B**) repeatability and (**C**) reproducibility of chitosan/GO/ion imprinting polymer (CS/GO/IIP) as an electrochemical sensor for Cu ((II) detection (50 μmol/L) [143].

Fartas et al. have employed graphene/gold nanoparticle/chitosan (GAuCS) nanocomposite films for glucose biosensing. The sensor was designed to immobilize glucose oxidase in thin films of GAuCS nanocomposites at gold electrodes [144]. Likewise, Casteleijn et al. used a simple spin-coating method to modify chitin-based biosensors on Au nanoparticles and polystyrene (PS). Due to chitin's solubility, this method opened a new domain of future possibilities [145]. The substantial binding of chitin has encouraged strong functionalization for the fabrication of biosensors. Hence, scientists have developed a novel $Co^{2+}$-metal-ion-based plasmon resonance surface sensor through chitin composites for enhanced sensitivity detection [146].

Besides, Ali et al. created a low-temperature $H_2S$ gas sensor using a conductive chitosan–CuO hybrid nanocomposite at different concentrations ranging from 1–9% vol-

ume/volume (*v*/*v*). The chitosan bio-nanocomposite resulted in a sufficiently flexible and transparent semiconductor. The detecting mechanism of the sensor occurs from proton transfer between the gas molecules and amino groups in the chitosan molecule. The presence of glycerol, i.e., OH groups, enhanced the formation of H-bonding [147].

Borgohain et al. have created a pollution sensor that helped to detect $Zn^{2+}$ and $Cu^{2+}$ ions at different concentrations in water. The co-precipitation method was utilized to make chitosan-ZnS quantum dot (QD) sensors. The formation of chitosan-ZnS QD tiny clusters was dependent on the concentration of metal ions in water, with a directly proportional relationship. As a result of the aggregated clusters, the absorption maxima occurred at longer wavelengths, and resulted in reduced energy [148].

### *4.3. Batteries and Electrochemistry*

LIBs have become important energy storage systems, especially in the usage of portable electronic devices. Their excellent properties, such as high energy density and low self-discharge rates, are repeatedly noticed [149]. As a result, comprehensive studies on novel electrode materials which are compatible with LIB electrolytes are highly crucial in the advancement of technologies [150].

Using a simple chitosan-assisted hydrothermal and subsequent calcination methods, Ma et al. have developed ultrathin $MoS_2$/graphene hetero-structures with high specific surface areas and efficient electrochemical characteristics [151]. Similarly, Chen et al. have introduced a N-doped carbon composite as a cathode material and CNT/chitosan as an amplified separator for innovative lithium–sulfur batteries (LSBs). This simple and effective method is expected to represent a watershed moment for the large-scale manufacturing of hetero-structures with a wide range of applications in batteries [152]. Moreover, Kim et al. have utilized a rGO/chitosan-based binder which has allowed significant improvement in the cycle stability and capacity of LSBs [153].

Other noteworthy and novel fabricated materials with high electrochemical properties among very recent works include a chitosan-solution-based Si@$SiO_2$@N-Carbon anode for LIBs [154], flexible chitosan-based carbon membranes as anodes for potassium- and sodium-ion batteries (KIBs/SIBs) [155], a chitosan-based N-doped carbon/$Li_2ZnTi_3O_8$/$TiO_2$ composite as an anode for LIBs [156], a chitosan-based C@$V_2O_5$ cathode for Zn-ion batteries (ZIBs) [157], a chitosan-based N-doped rGO/C@Si composite for LIBs as shown in Figure 9 [158] and novel S/Se/C supported by a chitosan-based interconnect with CNTs for novel lithium-chalcogenide batteries (NCBs) [159].

### *4.4. Fuel Cells*

Fuel cells modified with membranes via proton exchange have been displayed as a promising alternative in eco-friendly energy-related fields. The development of a highly conductive proton membrane is the most important aspect that determines the performance and efficiency of fuel cells [160]. To degrade chitin anaerobically, Li et al. created a microbial fuel cell using *Aeromonas hydrophila*. It was observed that the constructed fuel cell resulted in a seven times faster rate of chitin breakdown as compared to a conventional fermentation system [161]. Yang et al. introduced a low-cost Fe–N–C catalyst, resulting from an Fe(III)-chitosan hydrogel, to improve power generation in microbial fuel cells [162]. Thus, increased power generation was ensured. This approach allowed for the effective breakdown of resistant biomass in order to recover energy [163]. Researchers have reported a chitosan/rGO/polyaniline bio-nanocomposite to be a paradigm bio-anode for glucose-derived fuel cells. It exhibited excellent electrochemical properties with considerable stability [164]. Gorgieva et al. examined an effective chitosan-based N-doped rGO composite membrane for alkaline fuel cells. In this work, chitosan- and graphene-based homogenous materials were engineered using a variety of self-induced methods [165].

Furthermore, a cost-effective method was applied to assemble chitosan/montmorillonite nanocomposite using a ceramic support as an effective membrane for microbial fuel cells [166]. In another study, chitosan was cross-linked to poly(aminoanthraquinone)

nanocomposite which was a nitrogen-precursor-based Fe-N-C oxygen reduction catalyst for microbial fuel cells. The high-performance bio-anode in the fuel cell exhibited outstanding shape and retention characteristics due to its synergistic effects between porous structures [167]. This highly porous design along with anode materials have resulted in a 78-fold increase in maximum power density.

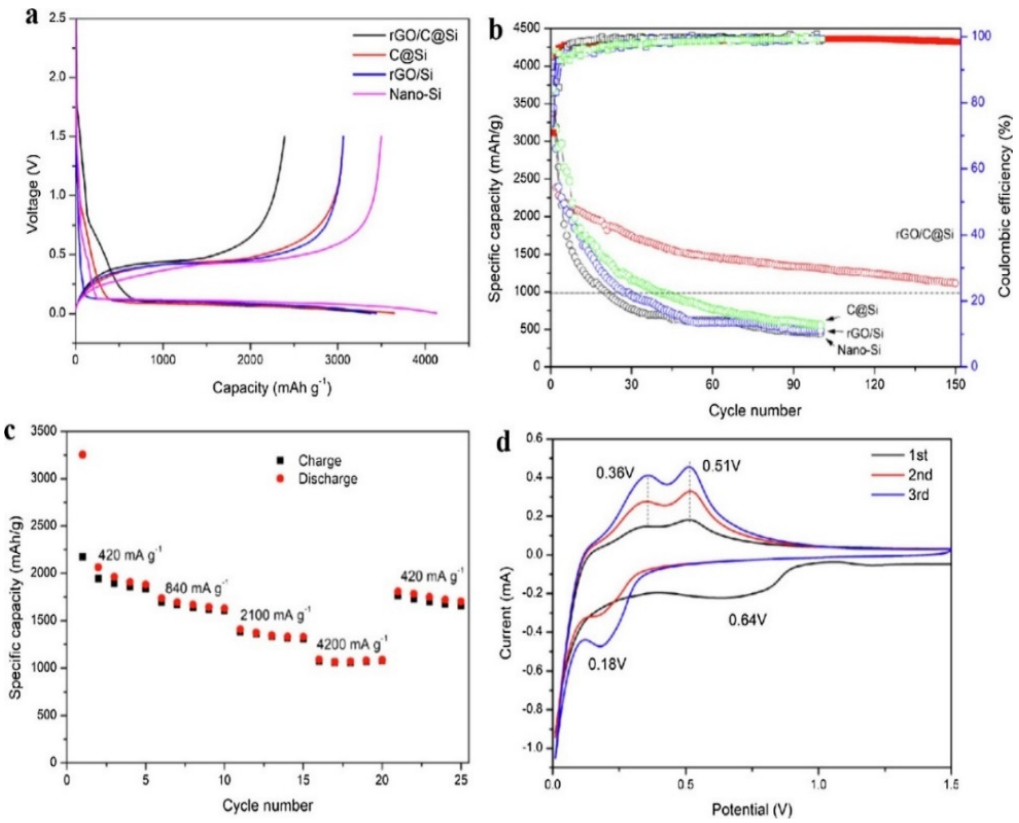


**Figure 9.** Electrochemical evaluations of fabricated anodes. (**a**) Initial charge/discharge of nano-Si, C@Si, rGO/Si and rGO/C@Si nanocomposites at a current density of 100 mA $g^{-1}$, (**b**) consistent current charge/discharge of nanocomposites and (**c**,**d**) rate performance and current/voltage profile of GO/C@Si anode [158].

Vijayalekshmi et al. created a cross-linked, flexible, oxidative and thermally stable chitosan-based green polymer electrolyte using methane, sulfonic acid and sodium-dodecylbenzene-sulfonic-acid-doped chitosan. At 100 °C, the polymer electrolyte had a conductivity of $4.67 \times 10^{-4}$ S/cm and thermal stability at a maximum value of 260 °C [167]. In short, this low-cost and eco-friendly technique ensures superior methanol barrier performance by reducing methanol absorption at higher methanol concentrations for fuel cells, as displayed in Figure 10 [168].

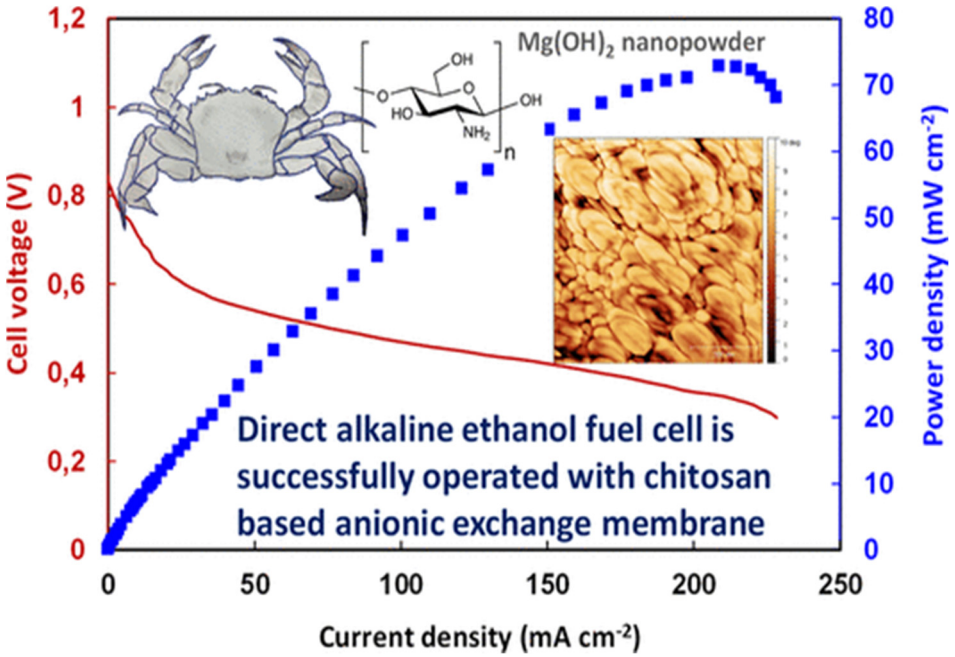


**Figure 10.** Novel polymer nanocomposite for alkaline fuel cells. Nanocomposite was fabricated using a solvent-casting method in which chitosan, GO, $Mg(OH)_2$ and benzyltrimethylammonium chloride were used [169].

Tohidian et al. applied a simple sol–gel technique to prepare chitosan-surface-modified CNT bio-nanocomposites. Additional benefits of chitosan-coated CNTs include a reduced danger of electronic short-circuiting and improved interaction between CNTs and chitosan, resulting in uniform dispersion [170]. Compared to pure chitosan membranes, bio-nanocomposites showed better thermal stability, proton conductivity and mechanical characteristics. Due to the electrostatic and hydrogen bonding between molecules, bio-nanocomposites achieved a power density of 98.5 mW $cm^{-2}$ at 70 °C [171]. Conversely, the reduced conductivity of protons was caused by the amino functional group, which led to less water uptake.

### *4.5. Supercapacitors*

Supercapacitors are a superior type of energy storage device. They exude higher capacitance, power density, durability cycle and stability. Many studies have been devoted to presenting novel nanomaterials as electrode materials from sustainable resources, due to their impressive electrochemical performance [122,172]. Recent research has been dedicated to produce chitosan-based bio-nanocomposites with remarkable properties, such as high power, an outstanding life cycle and an eco-friendly nature as compared to expensive nanoparticles [173,174].

A three-step technique which included the aerogel synthesis, aerogel carbonization and nitrogen self-doping processes was used to create chitosan-based supercapacitors for elevated enactment. This bio-nanocomposite showed a specific capacitance of 331 F $g^{-1}$ in 6 mol $L^{-1}$ using a KOH electrolyte at 1 A $g^{-1}$, with excellent stability of 90% after 10,000 cycles [175]. Major and noteworthy performance values were reached by preparing chitosan-based supercapacitors, which showed specific energy and power density at maximum recorded values of 10.46 Wh $kg^{-1}$ and 500.08 W $kg^{-1}$, respectively [176]. Similarly, Lin et al. have created a chitosan-based hydrogel using an ultrafast hydrogelation technique in which carboxylation of chitosan was carried out at 6, 8 and 10 values, thus producing a supramolecular electrolyte hydrogel with excellent specific capacitance of chitosan, chitosan-6, chitosan-8 and chitosan-10 supercapacitors at 35 F·$g^{-1}$, 72.5 F·$g^{-1}$, 49.2 F·$g^{-1}$ and 40.5 F·$g^{-1}$, respectively [177]. It was a facile and simple technology which has shown great potential for developing future bio-based supercapacitors.

### *4.6. Solar Cells*

Following cellulose, chitosan is the most abundant biomass-containing amino-polysac charide on earth. The ability of chitosan to produce a transparent film while maintaining its properties has influenced scientists' interest in designing solar cells [178]. The amine groups on the main chain of chitosan make it a viable option for cathode interlayers, while additional functionalization is added due to the hydroxyl and amino groups throughout the main chain [179].

Praveen et al. produced organic solar cells with a power conversion efficiency of 5.83% by utilizing layer-by-layer and self-assembled chitosan with a uniform and controllable nanoscale thickness [180]. The engineered solar cells exhibited higher efficiency due to their organized structural form, which produced both interfacial and molecule dipoles. The dipoles reduced the work function of electrodes, which has led to their promising and highly compatible utilization [181]. The self-assembled chitosan has improved performance up from 100 to 200% as compared to spin-coated chitosan interlayers and fuel cells. It was observed without any cathode interlayer, in terms of power conversion and efficacy, respectively (Figure 11) [182].

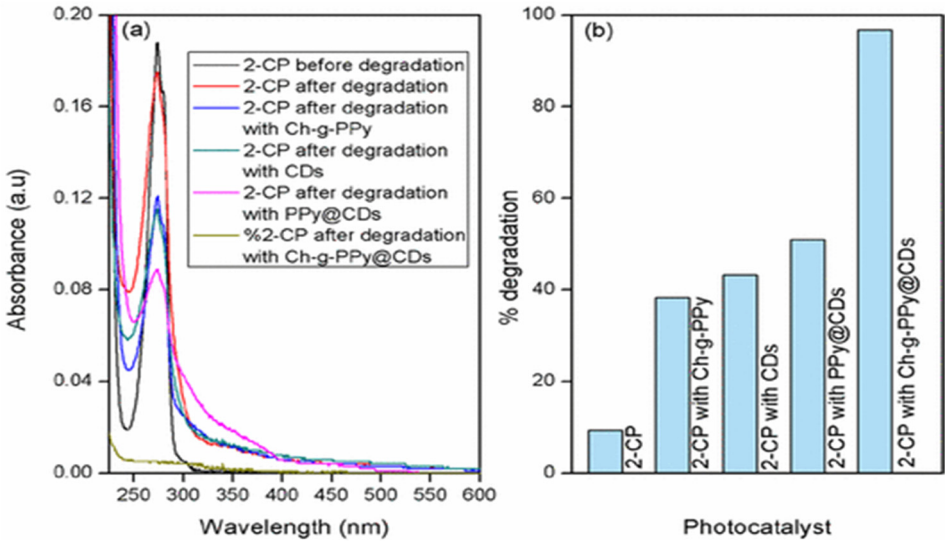


**Figure 11.** (**a**) Photocatalytic degradation of various nanomaterials via sunlight irradiation after 90 min, (**b**) efficiency of degradation comparing catalysts such as chitosan-grafted polypyrrole (Ch-g-PPy), polyrrole-based carbon dot (PPy@CD) and chiton-grafted polypyrrole carbon dot (Ch-g-PPy@CD) nanocomposites [183].

Moreover, Zulkifli et al. used a chitosan-based polymer electrolyte to create a high-performance plasmonic dye-sensitized solar cell [184]. Polyethene oxide (PEO) was placed between the $TiO_2$/dye photoelectrode and the Pt counter electrode in a chitosan-based solar cell. A simple solution-casting approach was used to add the ion donor NH4I salt. The mixing of chitosan with PEO was performed, which enhanced the flexibility of the electrolyte, the mobility of ions and the conductivity [185]. Thus, the 16.5 wt.% of chitosan and 38.5 wt.% of PEO:NH4I exhibited a significant increase in conductivity, respectively. The dye-sensitized solar cells (DSSC) recorded a 19-fold improvement of overall efficiency from 0.06% to 1.13% by incorporating $TiO_2$ particles into the cell system [186]. Table 2 summarizes chitosan/chitin-based nanomaterials, their mode of fabrication and utilization in energy-related applications.

**Table 2.** Tabulation of chitin/chitosan-based nanomaterials and their energetic applications.

| Composite Materials | Manufacturing Routes | Applications | Outcomes | Ref. |
|---|---|---|---|---|
| Semiconducting chitosan film | Casting method | $H_2S$ gas sensor | • Average min. response time of 14.9 ± 3.7 s with a 15 ppm detection limit | [147,187] |
| $Fe_3O_4$/chitosan | Chemical modification | Biosensor for gallic acid (GA) detection | • Detection limit of 12.1 nM<br>• Dynamic range of 0.5–300.0 µm | [188] |
| Ti–6Al–4V alloy coated with fumed silica/chitosan/poly(vinylpyrrolidone) composite | Artificial saliva solution | Coating for electrochemical corrosion | • Inhibition efficiency of 99.85% | [189] |
| Fe/chitosan-coated carbon electrode | Co-electrodeposition | Sensor for As(III) detection | • Recorded detection limits of 1.12 ppb and 1.01 ppb for mining wastewater and soil, respectively | [190] |
| Ag nanoparticles/chitosan-thiourea-formaldehyde | Polymeric metal complexation | Biosensor for non-enzymatic glucose detection | • Detection limit of 0.046 mM with 35.22 mA $mM^{-1}$ $cm^{-2}$ sensitivity | [191] |
| F-rGO @ CNTs/chitosan | Freeze-drying and dip-coating | Piezoresistive pressure sensor | • Response time of 170 ms and sensitivities of 4.97 $kPa^{-1}$ and 0.05 $kPa^{-1}$ in 0–3 kPa and 40–80 kPa, respectively | [192] |
| Chitosan/zinc oxide/single-walled CNTs | Solution casting | Chemiresistive humidity sensor | • Range of humidity detection of 11–97% | [193] |
| Copper ferrite nanoparticles/chitosan | Ultra-sonication | High-performance electrochemical | • Range of detection limit between 0.025–697.175 µM | [194] |
| Localized surface plasmon resonance (LSPR)-based optical fiber/chitosan-capped gold nanoparticles on BSA | Chemical modification | Optical fiber sensor for Hg(II) detection | • Limits of detection for water and seawater were 0.1 and 0.2 ppb, respectively | [195] |
| Graphene QDs/chitosan | Ultrasound dispersion | Humidity sensor | • High response sensitivity and short response/recovery time, i.e., 36 s/3 s | [196] |
| Polypyrrole/chitin nanofibers/carbon nanotubes | Vacuum filtration with freeze-drying | Supercapacitors | • 2 $Ag^{-1}$ records an 86.6% retention rate after 5000 cycles and 362 F $g^{-1}$ specific capacity at 5 $mVs^{-1}$ in 1 $molL^{-1}$ | [197] |
| Chitin/GO/zinc oxide/polyaniline | Co-polymerisation | Chitin-based polyaniline electrode for Cu(II) detection | • Response time of 240 s and detection limit of 13.77 ppm | [198] |
| Chitosan/cellulose acetate/PVA gel | Phase inversion and polymerisation | Supercapacitors | • Retention rate of 71.2% after 1000 cycles<br>• Specific capacitance of 5.5 $mFcm^{-1}$ at 20 $mVs^{-1}$ | [199] |
| MOF-5/chitosan | Chemical modification | High-performance supercapacitors | • Specific capacitance and capability rate records values of 199.9 F $g^{-1}$ and 75.6%, respectively | [200] |
| Polyionic liquid/carboxymethyl chitosan | Direct carbonization | Supercapacitors | • At 0.1 $Ag^{-1}$, specific capacitance of 633 F $g^{-1}$ and stability after 10,000 cycles | [201] |
| Chitosan/graphene/ionic liquid/ferrocene nanocomposite | Chemical modification and drop-coating | Electrochemical immunosensor | • Highly selective and sensitive to prostate-specific antigen and detection limit of $4.8 \times 10^{-8}$ ng $mL^{-1}$ | [202] |
| Polyaniline-grafted chitosan/GO-CNT/$Fe_3O_4$ nanocomposite | Solution mixing evaporation | Electrode material for supercapacitors | • Life cycle of 99.8%<br>• Specific capacitance at 100 $Ag^{-1}$ | [203] |
| Nano-cobalt/chitosan composite coating | Implantation | Electrochemical and $H_2$ evolution | • Resistance value of 1150.77 kΩ $cm^2$<br>• Nanocomposite coating up to 99.01% | [204] |
| Chitin from prawn shell/sodium dihydrogen citrate | Chemical extraction and drying in vacuum conditions | Batteries | • The stable discharge capacity of roughly 157 mAh $g^{-1}$ surpassing 15 cycles | [205] |
| Chitin fiber non-woven separator | Centrifugal jet spinning | Fuel cells | • Current discharge at ±200 µA | [206] |
| Sulfonated chitosan/GO | Casting | Direct methanol fuel cells | • Conductivity of $4.86 \times 10^{-3}$ $Scm^{-1}$ at (25 °C),<br>• Selectivity of $1.89 \times 10^5$ $Scm^{-3}$ s | [207] |

**Table 2.** *Cont.*

| Composite Materials | Manufacturing Routes | Applications | Outcomes | Ref. |
|---|---|---|---|---|
| Chitosan/GO on membrane substrates of sulfonated poly(vinylidenefluoride) | Sulfonation and alternate dipping | High-temperature proton exchange membrane fuel cells | • Conductivity values of $2.34 \times 10^{-1}$ S/cm and $1.56 \times 10^{-1}$ S/cm at 140 °C<br>• Methanol permeability was $(2.26–3.46) \times 10^{-7}$ $cm^2/s$<br>• Proton conductivity reached $2.34 \times 10^{-1}$ S/cm at 140 °C under anhydrous conditions | [208] |
| Chitosan/GO aerogel | Hydrothermal method | Microwave absorption | • Density value of 125 $cm^2/g$ and specific shielding effectiveness of ~−556 $dBcm^3/g$ | [209] |
| Chitosan/hydroxyl ethylcellulose/polyaniline loaded with GO doped by silver nanoparticles bio-nanocomposite as a hydrogel | Hydrothermal method | Efficient semiconductor material | • Hydrogels improved DC conductivity by about 25 times from $3.37 \times 10^{-3}$ to $8.53 \times 10^{-2}$ S/cm | [210] |
| Chitosan/ammonium thiocyanate | Solution-casting technique | Electric double-layer capacitor | • High ionic conductivity of $8.57 \times 10^{-4}$ S/cm was obtained | [211] |

## 5. Limitations and Challenges

The applications and merits of novel and promising biopolymers, i.e., chitin- and chitosan-based bio-nanocomposites are apparent to mitigate future global issues. Despite having outstanding biological and physiochemical characteristics, the molecule's flaws offer major hurdles and limits to its applicability in a variety of key industries. Therefore, several outlined disadvantages and problems must be addressed to ensure the modification of chitosan-based bio-nanocomposites. There are major thoughtful drawbacks which must be highlighted (Figure 12), and are outlined below:

- The current limitations in the medicinal fields are caused by low solubility and pH, which have led to instable physiological changes among nanocomposites.
- The hygiene and safety of synthesized bio-nanocomposites remain uncertain as the European Food Safety Authority (EFSA) denies them, despite possessing an approval for food contact from the Food Development Authority (FDA).
- Low colloidal stability makes chitin- and chitosan-based bio-nanocomposites unsuitable for large-scale drug delivery.
- Elevated elasticity of chitosan-based bio-nanocomposites restricts their use and applications.
- Despite showing satisfactory effectiveness in several medicinal applications, there are numerous issues such as drug release, loading efficacy and capacity, rate of degradation, and functionalization.
- Finally, industrial processing centers continue to face financial challenges in establishing a solid commercial viability of sustainable biopolymers in the real world.

*Future Recommendations*

The importance of chitosan-based nanocomposites is skyrocketing owing to their plentiful advantages. However, it does have some difficulties that must be overcome. The following section narrates some elements and suggestions for future study and research:

- Nanotechnology has great potential in agro-economics to improve agricultural areas. In this regard, nano-chitin or nano-chitosan might be powerful tools for delivering environmentally benign nano-chemicals or nano-agro-fertilizers.
- Their components can be used to grow crops, manage pests, increase fish output, produce meat, preserve seeds, improve the immune system of crops and develop crops with high drought and salinity resistance, among other elements.
- There are very few in vivo studies demonstrating the formulation and conjugation of chitosan-based nano-carriers with antibodies as well as the assessment of long-term toxicity of the nano-carriers. Thus, future research can be conducted on studies of antibodies coupled with chitosan-based nano-carriers.

- As metal oxides have shown unique semiconducting, optical and photocatalytic characteristics, chitosan/metal oxide bio-nanocomposites could bring a remarkable change for wound healing and other future regeneration studies.
- Chitin and chitosan can be an attractive future research choice as heterogeneous bio-nanocatalysts and kinetic studies.
- Due to their physiological pH, chitosan-based bio-nanocomposites have limited solubility. In this situation, researchers should concentrate on developing novel chitosan-based bio-nanocomposite materials with improved solubility and aggregation.
- Conventional acid and alkali treatments should be replaced with novel biological methods for chitosan extraction. In competitive industrial situations, eco-friendly and cost-effective extraction methods must also be established.
- Crabs, shrimps, insects and fungi are acquiring enormous demand in many industrial areas due to their remarkable characteristics. As these natural resources become more popular, there is a growing worry that they will become extinct. The researchers' mission should be focused on identifying alternate sources of energy in order to restore ecological equilibrium.
- Researchers should concentrate on introducing nanomaterials with high degrees of elasticity for novel electronic devices.

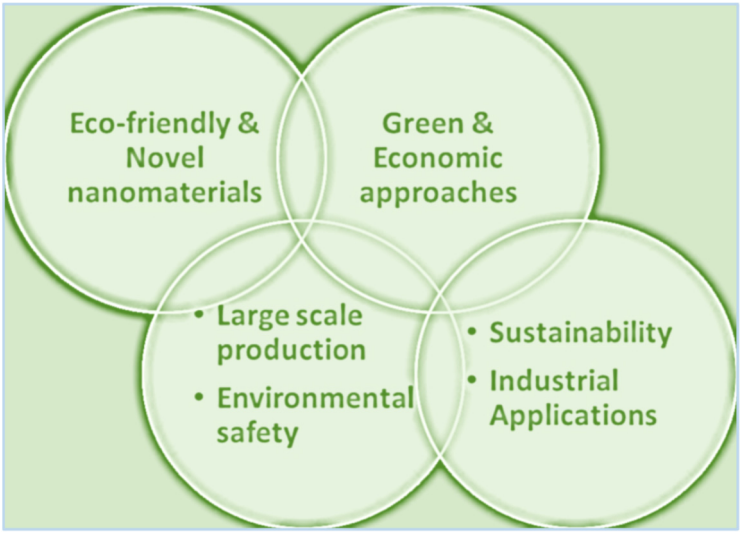


**Figure 12.** Future perspectives.

## 6. Conclusions

To summarize, the hazardous impact of toxic and non-biodegradable materials has caused adverse effects on human health and the environment. Consequently, it has indeed seized the attention of researchers to introduce a variety of bio-nanocomposites. Currently, chitin- and chitosan-derived bio-nanocomposites are the emerging alternates with outstanding functional properties and compatibility. Herein, we have summarized their structural analysis and fabrication into a large number of graphene-based bio-nanocomposites. It was observed that several types of fabrication methods have been utilized which impart different properties for their particular applications. In particular, progressive trends of energetic applications have been elaborated with their impressive attributes towards electronic devices. Finally, we conclude that chitosan-derived graphene bio-nanocomposites have a strong potential for unexplored applications, such as wastewater treatment and environmental pollution, as well as within the oil and gas industry, such as for drilling fluids, mechanical operations, kinetic and computational chemistry.

**Author Contributions:** R.I., original concept and initial draft of the paper; R.I. and G.K., summary of the literature; G.K., M.M.S. and A.S., processing and data analysis; B.M.J. and M.A.Q., supervised and coordinated the work; G.K., M.M.S. and R.I., funding acquisition. All authors have read and agreed to the published version of the manuscript.

**Funding:** The authors would like to gratefully acknowledge the Malaysia–Thailand Joint Authority under grant number IF062-2019 and the Fundamental Research Grant Scheme FP050-2019A from the University of Malaya for providing funds during the course of this study. Finally, this work was co-financed by the European Union and Greek national funds through the Competitiveness, Entrepreneurship and Innovation operation program, under the call RESEARCH–CREATE–INNOVATE (second cycle); acronym: SEMI-WEB; project code: T2EDK-02073.

**Institutional Review Board Statement:** Not applicable.

**Informed Consent Statement:** Not applicable.

**Data Availability Statement:** Not applicable.

**Conflicts of Interest:** The authors declare that there are no conflicts of interest regarding the publication of this manuscript.

## References

1. Haupt, K.; Medina Rangel, P.X.; Bui, B.T.S. Molecularly imprinted polymers: Antibody mimics for bioimaging and therapy. *Chem. Rev.* **2020**, *120*, 9554–9582. [CrossRef] [PubMed]
2. Saska, S.; Pilatti, L.; Blay, A.; Shibli, J.A. Bioresorbable Polymers: Advanced Materials and 4D Printing for Tissue Engineering. *Polymers* **2021**, *13*, 563. [CrossRef] [PubMed]
3. Xia, Y.; He, Y.; Zhang, F.; Liu, Y.; Leng, J. A review of shape memory polymers and composites: Mechanisms, materials, and applications. *Adv. Mater.* **2021**, *33*, 2000713. [CrossRef]
4. Yu, Y.; Shen, M.; Song, Q.; Xie, J. Biological activities and pharmaceutical applications of polysaccharide from natural resources: A review. *Carbohydr. Polym.* **2018**, *183*, 91–101. [CrossRef] [PubMed]
5. Bajpai, A.K.; Shukla, S.K.; Bhanu, S.; Kankane, S. Responsive polymers in controlled drug delivery. *Prog. Polym. Sci.* **2008**, *33*, 1088–1118. [CrossRef]
6. Balint, R.; Cassidy, N.J.; Cartmell, S.H. Conductive polymers: Towards a smart biomaterial for tissue engineering. *Acta Biomater.* **2014**, *10*, 2341–2353. [CrossRef]
7. Zhu, Y.; Romain, C.; Williams, C.K. Sustainable polymers from renewable resources. *Nature* **2016**, *540*, 354–362. [CrossRef]
8. Wang, X.; Yao, C.; Wang, F.; Li, Z. Cellulose-based nanomaterials for energy applications. *Small* **2017**, *13*, 1702240. [CrossRef]
9. Xue, G.; Xu, Y.; Ding, T.; Li, J.; Yin, J.; Fei, W.; Cao, Y.; Yu, J.; Yuan, L.; Gong, L.; et al. Water-evaporation-induced electricity with nanostructured carbon materials. *Nat. Nanotechnol.* **2017**, *12*, 317–321. [CrossRef]
10. Inagaki, M.; Toyoda, M.; Soneda, Y.; Morishita, T. Nitrogen-doped carbon materials. *Carbon* **2018**, *132*, 104–140. [CrossRef]
11. Mohan, M.; Sharma, V.K.; Kumar, E.A.; Gayathri, V. Hydrogen storage in carbon materials—A review. *Energy Storage* **2019**, *1*, e35. [CrossRef]
12. Papageorgiou, D.G.; Kinloch, I.A.; Young, R.J. Mechanical properties of graphene and graphene-based nanocomposites. *Prog. Mater. Sci.* **2017**, *90*, 75–127. [CrossRef]
13. Wu, J.B.; Lin, M.L.; Cong, X.; Liu, H.N.; Tan, P.H. Raman spectroscopy of graphene-based materials and its applications in related devices. *Chem. Soc. Rev.* **2018**, *47*, 1822–1873. [CrossRef]
14. Rinaudo, M. Main properties and current applications of some polysaccharides as biomaterials. *Polym. Int.* **2008**, *57*, 397–430. [CrossRef]
15. Bertolino, V.; Cavallaro, G.; Milioto, S.; Lazzara, G. Polysaccharides/Halloysite nanotubes for smart bionanocomposite materials. *Carbohydr. Polym.* **2020**, *245*, 116502. [CrossRef]
16. Malerba, M.; Cerana, R. Chitin- and Chitosan-Based Derivatives in Plant Protection against Biotic and Abiotic Stresses and in Recovery of Contaminated Soil and Water. *Polysaccharides* **2020**, *1*, 21–30. [CrossRef]
17. Rinaudo, M. Chitin and chitosan: Properties and applications. *Prog. Polym. Sci.* **2006**, *31*, 603–632. [CrossRef]
18. Pacheco, N.; Naal-Ek, M.G.; Ayora-Talavera, T.; Shirai, K.; Román-Guerrero, A.; Fabela-Morón, M.F.; Cuevas-Bernardino, J.C. Effect of bio-chemical chitosan and gallic acid into rheology and physicochemical properties of ternary edible films. *Int. J. Biol. Macromol.* **2019**, *125*, 149–158. [CrossRef]
19. Anitha, A.; Sowmya, S.; Kumar, P.S.; Deepthi, S.; Chennazhi, K.P.; Ehrlich, H.; Tsurkan, M.; Jayakumar, R. Chitin and chitosan in selected biomedical applications. *Prog. Polym. Sci.* **2014**, *39*, 1644–1667. [CrossRef]
20. López-Mata, M.A.; Ruiz-Cruz, S.; Silva-Beltrán, N.P.; Ornelas-Paz, J.D.J.; Ocaño-Higuera, V.M.; Rodríguez-Félix, F.; Cira-Chávez, L.A.; Del-Toro-Sánchez, C.L.; Shirai, K. Physicochemical and antioxidant properties of chitosan films incorporated with cinnamon oil. *Int. J. Polym. Sci.* **2015**, *2015*, 1–8. [CrossRef]

21. Espadín, A.; De Dios, L.T.; Ruvalcaba, E.; Valadez-García, J.; Velasquillo, C.; Bustos-Jaimes, I.; Vázquez-Torres, H.; Gimeno, M.; Shirai, K. Production and characterization of a nanocomposite of highly crystalline nanowhiskers from biologically extracted chitin in enzymatic poly (ε-caprolactone). *Carbohydr. Polym.* **2018**, *181*, 684–692. [CrossRef]
22. Sirajudheen, P.; Poovathumkuzhi, N.C.; Vigneshwaran, S.; Chelaveettil, B.M.; Meenakshi, S. Applications of chitin and chitosan based biomaterials for the adsorptive removal of textile dyes from water-A comprehensive review. *Carbohydr. Polym.* **2021**, *273*, 118604. [CrossRef]
23. Safarzadeh, M.; Sadeghi, S.; Azizi, M.; Rastegari-Pouyani, M.; Pouriran, R.; Hoseini, M.H.M. Chitin and chitosan as tools to combat COVID-19: A triple approach. *Int. J. Biol. Macromol.* **2021**, *183*, 235–244. [CrossRef] [PubMed]
24. Babaei-Ghazvini, A.; Acharya, B.; Korber, D.R. Antimicrobial Biodegradable Food Packaging Based on Chitosan and Metal/Metal-Oxide Bio-Nanocomposites: A Review. *Polymers* **2021**, *13*, 2790. [CrossRef] [PubMed]
25. Vedula, S.S.; Yadav, G.D. Chitosan-Based Membranes Preparation and Applications: Challenges and Opportunities. *J. Indian Chem. Soc.* **2021**, *98*, 100017. [CrossRef]
26. Ndlovu, S.P.; Ngece, K.; Alven, S.; Aderibigbe, B.A. Gelatin-Based Hybrid Scaffolds: Promising Wound Dressings. *Polymers* **2021**, *13*, 2959. [CrossRef] [PubMed]
27. Khan, A.; Alamry, K.A. Recent advances of emerging green chitosan-based biomaterials with potential biomedical applications: A review. *Carbohydr. Res.* **2021**, *506*, 108368. [CrossRef] [PubMed]
28. Pal, P.; Pal, A.; Nakashima, K.; Yadav, B.K. Applications of chitosan in environmental remediation: A review. *Chemosphere* **2020**, *266*, 128934. [CrossRef]
29. Jariwala, D.; Sangwan, V.K.; Lauhon, L.J.; Marks, T.J.; Hersam, M.C. Carbon nanomaterials for electronics, optoelectronics, photovoltaics, and sensing. *Chem. Soc. Rev.* **2013**, *42*, 2824–2860. [CrossRef]
30. Ikram, R.; Jan, B.M.; Ahmad, W. An overview of industrial scalable production of graphene oxide and analytical approaches for synthesis and characterization. *J. Mater. Res. Technol.* **2020**, *9*, 11587–11610. [CrossRef]
31. Novoselov, K.S.; Geim, A.K.; Morozov, S.V.; Jiang, D.E.; Zhang, Y.; Dubonos, S.V.; Grigorieva, I.V.; Firsov, A.A. Electric field effect in atomically thin carbon films. *Science* **2004**, *306*, 666–669. [CrossRef]
32. Ikram, R.; Jan, B.M.; Ahmad, W. Advances in synthesis of graphene derivatives using industrial wastes precursors; prospects and challenges. *J. Mater. Res. Technol.* **2020**, *9*, 15924–15951. [CrossRef]
33. Azizi-Lalabadi, M.; Jafari, S.M. Bio-nanocomposites of graphene with biopolymers; fabrication, properties, and applications. *Adv. Colloid Interface Sci.* **2021**, *292*, 102416. [CrossRef]
34. Tiwari, S.K.; Sahoo, S.; Wang, N.; Huczko, A. Graphene research and their outputs: Status and prospect. *J. Sci. Adv. Mater. Devices* **2020**, *5*, 10–29. [CrossRef]
35. Olabi, A.G.; Abdelkareem, M.A.; Wilberforce, T.; Sayed, E.T. Application of graphene in energy storage device–A review. *Renew. Sustain. Energy Rev.* **2021**, *135*, 110026. [CrossRef]
36. Balandin, A.A. Phononics of graphene and related materials. *ACS Nano* **2020**, *14*, 5170–5178. [CrossRef] [PubMed]
37. Huang, H.; Shi, H.; Das, P.; Qin, J.; Li, Y.; Wang, X.; Su, F.; Wen, P.; Li, S.; Lu, P.; et al. The chemistry and promising applications of graphene and porous graphene materials. *Adv. Funct. Mater.* **2020**, *30*, 1909035. [CrossRef]
38. Tarcan, R.; Todor-Boer, O.; Petrovai, I.; Leordean, C.; Astilean, S.; Botiz, I. Reduced graphene oxide today. *J. Mater. Chem. C* **2020**, *8*, 1198–1224. [CrossRef]
39. Ahmad, W.; Ur Rahman, A.; Ahmad, I.; Yaseen, M.; Mohamed Jan, B.; Stylianakis, M.M.; Kenanakis, G.; Ikram, R. Oxidative Desulfurization of Petroleum Distillate Fractions Using Manganese Dioxide Supported on Magnetic Reduced Graphene Oxide as Catalyst. *Nanomaterials* **2021**, *11*, 203. [CrossRef] [PubMed]
40. Ikram, R.; Mohamed Jan, B.; Vejpravova, J.; Choudhary, M.I.; Zaman Chowdhury, Z. Recent Advances of Graphene-Derived Nanocomposites in Water-Based Drilling Fluids. *Nanomaterials* **2020**, *10*, 2004. [CrossRef] [PubMed]
41. Sun, Z.; Fang, S.; Hu, Y.H. 3D Graphene materials: From understanding to design and synthesis control. *Chem. Rev.* **2020**, *120*, 10336–10453. [CrossRef]
42. Kumar, R.; Sahoo, S.; Joanni, E.; Singh, R.K.; Maegawa, K.; Tan, W.K.; Kawamura, G.; Kar, K.K.; Matsuda, A. Heteroatom doped graphene engineering for energy storage and conversion. *Mater. Today* **2020**, *39*, 47–65. [CrossRef]
43. Wang, W.; Meng, Q.; Li, Q.; Liu, J.; Zhou, M.; Jin, Z.; Zhao, K. Chitosan derivatives and their application in biomedicine. *Int. J. Mol. Sci.* **2020**, *21*, 487. [CrossRef]
44. Kumar, M.R.; Muzzarelli, R.; Muzzarelli, C.; Sashiwa, H.; Domb, A.J. Chitosan chemistry and pharmaceutical perspectives. *Chem. Rev.* **2004**, *104*, 6017–6084. [CrossRef]
45. Shariatinia, Z. Pharmaceutical applications of chitosan. *Adv. Colloid Interface Sci.* **2019**, *263*, 131–194. [CrossRef]
46. Sahariah, P.; Masson, M. Antimicrobial chitosan and chitosan derivatives: A review of the structure—Activity relationship. *Biomacromolecules* **2017**, *18*, 3846–3868. [CrossRef]
47. Cheung, R.C.F.; Ng, T.B.; Wong, J.H.; Chan, W.Y. Chitosan: An update on potential biomedical and pharmaceutical applications. *Mar. Drugs* **2015**, *13*, 5156–5186. [CrossRef] [PubMed]
48. Choi, C.; Nam, J.P.; Nah, J.W. Application of chitosan and chitosan derivatives as biomaterials. *J. Ind. Eng. Chem.* **2016**, *33*, 1–10. [CrossRef]
49. Zhang, L.; Zeng, Y.; Cheng, Z. Removal of heavy metal ions using chitosan and modified chitosan: A review. *J. Mol. Liq.* **2016**, *214*, 175–191. [CrossRef]

50. Cavallaro, G.; Micciulla, S.; Chiappisi, L.; Lazzara, G. Chitosan-based smart hybrid materials: A physico-chemical perspective. *J. Mater. Chem. B* **2021**, *9*, 594–611. [CrossRef] [PubMed]
51. Karimi-Maleh, H.; Ayati, A.; Davoodi, R.; Tanhaei, B.; Karimi, F.; Malekmohammadi, S.; Orooji, Y.; Fu, L.; Sillanpää, M. Recent advances in using of chitosan-based adsorbents for removal of pharmaceutical contaminants: A review. *J. Clean. Prod.* **2021**, 125880. [CrossRef]
52. Si, Z.; Hou, Z.; Vikhe, Y.S.; Thappeta, K.R.V.; Marimuthu, K.; De, P.P.; Ng, O.T.; Li, P.; Zhu, Y.; Pethe, K.; et al. Antimicrobial effect of a novel chitosan derivative and its synergistic effect with antibiotics. *ACS Appl. Mater. Interfaces* **2021**, *13*, 3237–3245. [CrossRef] [PubMed]
53. Brasselet, C.; Pierre, G.; Dubessay, P.; Dols-Lafargue, M.; Coulon, J.; Maupeu, J.; Vallet-Courbin, A.; de Baynast, H.; Doco, T.; Michaud, P.; et al. Modification of Chitosan for the Generation of Functional Derivatives. *Appl. Sci.* **2019**, *9*, 1321. [CrossRef]
54. Zhou, D.Y.; Wu, Z.X.; Yin, F.W.; Song, S.; Li, A.; Zhu, B.W.; Yu, L.L. Chitosan and Derivatives: Bioactivities and Application in Foods. *Annu. Rev. Food Sci. Technol.* **2021**, *12*, 407–432. [CrossRef]
55. Simsir, H.; Eltugral, N.; Karagoz, S. Hydrothermal carbonization for the preparation of hydrochars from glucose, cellulose, chitin, chitosan and wood chips via low-temperature and their characterization. *Bioresour. Technol.* **2017**, *246*, 82–87. [CrossRef]
56. Hu, K.; Kulkarni, D.D.; Choi, I.; Tsukruk, V.V. Graphene-polymer nanocomposites for structural and functional applications. *Prog. Polym. Sci.* **2014**, *39*, 1934–1972. [CrossRef]
57. Sun, X.; Huang, C.; Wang, L.; Liang, L.; Cheng, Y.; Fei, W.; Li, Y. Recent progress in graphene/polymer nanocomposites. *Adv. Mater.* **2021**, *33*, 2001105. [CrossRef]
58. Cui, Y.; Kundalwal, S.I.; Kumar, S. Gas barrier performance of graphene/polymer nanocomposites. *Carbon* **2016**, *98*, 313–333. [CrossRef]
59. Guan, L.Z.; Zhao, L.; Wan, Y.J.; Tang, L.C. Three-dimensional graphene-based polymer nanocomposites: Preparation, properties and applications. *Nanoscale* **2018**, *10*, 14788–14811. [CrossRef] [PubMed]
60. Sanes, J.; Sánchez, C.; Pamies, R.; Avilés, M.D.; Bermúdez, M.D. Extrusion of polymer nanocomposites with graphene and graphene derivative nanofillers: An overview of recent developments. *Materials* **2020**, *13*, 549. [CrossRef]
61. Singh, K.; Ohlan, A.; Dhawan, S.K. Polymer-graphene nanocomposites: Preparation, characterization, properties, and applications. In *Nanocomposites—New Trends and Developments*; Ebrahimi, F., Ed.; InTech: Rijeka, Croatia, 2012; Chapter 3; pp. 37–72.
62. Papageorgiou, D.G.; Li, Z.; Liu, M.; Kinloch, I.A.; Young, R.J. Mechanisms of mechanical reinforcement by graphene and carbon nanotubes in polymer nanocomposites. *Nanoscale* **2020**, *12*, 2228–2267. [CrossRef] [PubMed]
63. Zhang, D.; Zhang, K.; Wang, Y.; Wang, Y.; Yang, Y. Thermoelectric effect induced electricity in stretchable graphene-polymer nanocomposites for ultrasensitive self-powered strain sensor system. *Nano Energy* **2019**, *56*, 25–32. [CrossRef]
64. Xia, X.; Wang, Y.; Zhong, Z.; Weng, G.J. A frequency-dependent theory of electrical conductivity and dielectric permittivity for graphene-polymer nanocomposites. *Carbon* **2017**, *111*, 221–230. [CrossRef]
65. Huang, G.; Chen, W.; Wu, T.; Guo, H.; Fu, C.; Xue, Y.; Wang, K.; Song, P. Multifunctional graphene-based nano-additives toward high-performance polymer nanocomposites with enhanced mechanical, thermal, flame retardancy and smoke suppressive properties. *Chem. Eng. J.* **2021**, *410*, 127590. [CrossRef]
66. Wang, J.; Jin, X.; Li, C.; Wang, W.; Wu, H.; Guo, S. Graphene and graphene derivatives toughening polymers: Toward high toughness and strength. *Chem. Eng. J.* **2019**, *370*, 831–854. [CrossRef]
67. Govindaraj, P.; Fox, B.; Aitchison, P.; Hameed, N. A review on graphene polymer nanocomposites in harsh operating conditions. *Ind. Eng. Chem. Res.* **2019**, *58*, 17106–17129. [CrossRef]
68. Zhang, M.; Li, Y.; Su, Z.; Wei, G. Recent advances in the synthesis and applications of graphene–polymer nanocomposites. *Polym. Chem.* **2015**, *6*, 6107–6124. [CrossRef]
69. Kang, H.; Tang, Y.; Yao, L.; Yang, F.; Fang, Q.; Hui, D. Fabrication of graphene/natural rubber nanocomposites with high dynamic properties through convenient mechanical mixing. *Compos. Part B Eng.* **2017**, *112*, 1–7. [CrossRef]
70. Bhattacharya, M. Polymer nanocomposites—A comparison between carbon nanotubes, graphene, and clay as nanofillers. *Materials* **2016**, *9*, 262. [CrossRef]
71. Shen, X.; Zheng, Q.; Kim, J.K. Rational design of two-dimensional nanofillers for polymer nanocomposites toward multifunctional applications. *Prog. Mater. Sci.* **2021**, *115*, 100708. [CrossRef]
72. Khodakarami, M.; Bagheri, M. Recent advances in synthesis and application of polymer nanocomposites for water and wastewater treatment. *J. Clean. Prod.* **2021**, *296*, 126404. [CrossRef]
73. Chaurasia, A.; Parashar, A. Effect of BNNR on mechanical properties of polyethylene nanocomposites. *Mater. Today Proc.* **2021**. [CrossRef]
74. Silva, M.; Pinho, I.S.; Covas, J.A.; Alves, N.M.; Paiva, M.C. 3D printing of graphene-based polymeric nanocomposites for biomedical applications. *Funct. Compos. Mater.* **2021**, *2*, 1–21.
75. Salimikia, I.; Heydari, R.; Yazdankhah, F. Polyaniline/graphene oxide nanocomposite as a sorbent for extraction and determination of nicotine using headspace solid-phase microextraction and gas chromatography–flame ionization detector. *J. Iran. Chem. Soc.* **2018**, *15*, 1593–1601. [CrossRef]
76. Heydari, M.; Saraji, M.; Jafari, M.T. Electrochemically prepared three-dimensional reduced graphene oxide-polyaniline nanocomposite as a solid-phase microextraction coating for ethion determination. *Talanta* **2020**, *209*, 120576. [CrossRef] [PubMed]

77. Suvina, V.; Krishna, S.M.; Nagaraju, D.H.; Melo, J.S.; Balakrishna, R.G. Polypyrrole-reduced graphene oxide nanocomposite hydrogels: A promising electrode material for the simultaneous detection of multiple heavy metal ions. *Mater. Lett.* **2018**, *232*, 209–212. [CrossRef]
78. Park, I.H.; Lee, J.Y.; Ahn, S.J.; Choi, H.J. Melt Rheology and Mechanical Characteristics of Poly (Lactic Acid)/Alkylated Graphene Oxide Nanocomposites. *Polymers* **2020**, *12*, 2402. [CrossRef]
79. Jasmi, F.; Azeman, N.H.; Bakar, A.A.A.; Zan, M.S.D.; Badri, K.H.; Su'ait, M.S. Ionic conductive polyurethane-graphene nanocomposite for performance enhancement of optical fiber Bragg grating temperature sensor. *IEEE Access* **2018**, *6*, 47355–47363. [CrossRef]
80. Jin, K.; Zhang, W.; Wang, Y.; Guo, X.; Chen, Z.; Li, L.; Zhang, Y.; Wang, Z.; Chen, J.; Sun, L.; et al. In–situ hybridization of polyaniline nanofibers on functionalized reduced graphene oxide films for high-performance supercapacitor. *Electrochim. Acta* **2018**, *285*, 221–229. [CrossRef]
81. Wan, Y.; Li, J.; Yang, Z.; Ao, H.; Xiong, L.; Luo, H. Simultaneously depositing polyaniline onto bacterial cellulose nanofibers and graphene nanosheets toward electrically conductive nanocomposites. *Curr. Appl. Phys.* **2018**, *18*, 933–940. [CrossRef]
82. Lu, B.; Yuan, X.; Ren, Y.; Shi, Q.; Wang, S.; Dong, J.; Nan, Z.D. Cost-effective three dimensional Ag/polymer dyes/graphene-carbon spheres hybrids for high performance nonenzymatic sensor and its application in living cell H2O2 detection. *Bioelectrochemistry* **2018**, *123*, 103–111. [CrossRef] [PubMed]
83. Wang, J.; Li, Q.; Peng, C.; Shu, N.; Niu, L.; Zhu, Y. To increase electrochemical performance of electrode material by attaching activated carbon particles on reduced graphene oxide sheets for supercapacitor. *J. Power Sources* **2020**, *450*, 227611. [CrossRef]
84. Hossain, M.F.; Park, J.Y. Plain to point network reduced graphene oxide-activated carbon composites decorated with platinum nanoparticles for urine glucose detection. *Sci. Rep.* **2016**, *6*, 1–10. [CrossRef] [PubMed]
85. Abd Muain, M.F.; Cheo, K.H.; Omar, M.N.; Hamzah, A.S.A.; Lim, H.N.; Salleh, A.B.; Tan, W.S.; Tajudin, A.A. Gold nanoparticle-decorated reduced-graphene oxide targeting anti hepatitis B virus core antigen. *Bioelectrochemistry* **2018**, *122*, 199–205. [CrossRef]
86. Van Pham, T. One-step hydrothermal synthesis and photocatalytic activity of $SnO_2$/rGO nanocomposites: Effects of pH values. *Commun. Phys.* **2021**, *31*.
87. Lawal, A.T. Graphene-based nano composites and their applications. A review. *Biosens. Bioelectron.* **2019**, *141*, 111384. [CrossRef]
88. Borah, M.J.; Devi, A.; Saikia, R.A.; Deka, D. Biodiesel production from waste cooking oil catalyzed by in-situ decorated $TiO_2$ on reduced graphene oxide nanocomposite. *Energy* **2018**, *158*, 881–889. [CrossRef]
89. Anichini, C.; Samorì, P. Graphene-Based Hybrid Functional Materials. *Small* **2021**, *17*, 2100514. [CrossRef]
90. Chen, T.; Zhou, Y.; Zhang, J.; Cao, Y. Two-dimensional $MnO_2$/reduced graphene oxide nanosheet as a high-capacity and high-rate cathode for lithium-ion batteries. *Int. J. Electrochem. Sci.* **2018**, *13*, 8575–8588. [CrossRef]
91. Chou, C.T.; Wang, F.H. Fabrication and characterization of transparent conducting reduced graphene oxide/Ag nanowires/ZnO: Ga composite thin films on flexible substrates. *J. Vac. Sci. Technol. A Vac. Surf. Film.* **2018**, *36*, 05G504. [CrossRef]
92. Gulati, U.; Chinna Rajesh, U.; Rawat, D.S. Reduced Graphene oxide supported copper oxide nanocomposites from a renewable copper mineral precursor: A green approach for decarboxylative C (sp3)–H activation of proline amino acid to afford value-added synthons. *ACS Sustain. Chem. Eng.* **2018**, *6*, 10039–10051. [CrossRef]
93. Huang, W.; Ding, S.; Chen, Y.; Hao, W.; Lai, X.; Peng, J.; Tu, J.; Cao, Y.; Li, X. 3D NiO hollow sphere/reduced graphene oxide composite for high-performance glucose biosensor. *Sci. Rep.* **2017**, *7*, 1–11. [CrossRef] [PubMed]
94. Wang, Y.; Mao, P.; Yan, F.; Gao, C.; Liu, Y.; Ding, J.; Wu, W.; Liu, Y. Flower-like $Fe_2O_3$/reduced graphene oxide composite for electrochemical energy storage. *Synth. Met.* **2016**, *222*, 198–204. [CrossRef]
95. Qian, L.; Wei, Z.; Yu, T.; Chang, B.; Wang, Z.; Liu, Y.; Sun, H.; Huang, W. Boosting the Electrocatalytic Hydrogen Evolution and Sodium-Storage Properties of Co9S8 Nanoparticles via the Encapsulation with Nitrogen-Doped Few-Layer Graphene Networks. *Sustain. Energy Fuels* **2021**, *5*, 4618–4627. [CrossRef]
96. Xuan, X.; Kim, J.Y.; Hui, X.; Das, P.S.; Yoon, H.S.; Park, J.Y. A highly stretchable and conductive 3D porous graphene metal nanocomposite based electrochemical-physiological hybrid biosensor. *Biosens. Bioelectron.* **2018**, *120*, 160–167. [CrossRef] [PubMed]
97. Zheng, L.; Zheng, H.; Huo, D.; Wu, F.; Shao, L.; Zheng, P.; Jiang, Y.; Zheng, X.; Qiu, X.; Liu, Y.; et al. N-doped graphene-based copper nanocomposite with ultralow electrical resistivity and high thermal conductivity. *Sci. Rep.* **2018**, *8*, 1–7.
98. Liu, Z.; Guo, Y. Sensitive determination of trace 4-nitrophenol in water based on thio-β-cyclodextrin functionalized graphene/copper nanospheres. *J. Electroanal. Chem.* **2018**, *825*, 57–64. [CrossRef]
99. Fan, H.; Wang, L.; Zhao, K.; Li, N.; Shi, Z.; Ge, Z.; Jin, Z. Fabrication, mechanical properties, and biocompatibility of graphene-reinforced chitosan composites. *Biomacromolecules* **2010**, *11*, 2345–2351. [CrossRef]
100. Sayyar, S.; Murray, E.; Thompson, B.C.; Chung, J.; Officer, D.L.; Gambhir, S.; Spinks, G.M.; Wallace, G.G. Processable conducting graphene/chitosan hydrogels for tissue engineering. *J. Mater. Chem. B* **2015**, *3*, 481–490. [CrossRef]
101. Liu, B.; Lian, H.T.; Yin, J.F.; Sun, X.Y. Dopamine molecularly imprinted electrochemical sensor based on graphene–Chitosan composite. *Electrochim. Acta* **2012**, *75*, 108–114. [CrossRef]
102. Kim, D.S.; Dhand, V.; Rhee, K.Y.; Park, S.J. Study on the effect of silanization and improvement in the tensile behavior of graphene-chitosan-composite. *Polymers* **2015**, *7*, 527–551. [CrossRef]
103. Fan, L.; Luo, C.; Li, X.; Lu, F.; Qiu, H.; Sun, M. Fabrication of novel magnetic chitosan grafted with graphene oxide to enhance adsorption properties for methyl blue. *J. Hazard. Mater.* **2012**, *215*, 272–279. [CrossRef] [PubMed]

104. Geng, L.; Lin, Y.; Chen, S.; Shi, S.; Cai, Y.; Li, L.; Peng, X. Superior strength and toughness of graphene/chitosan fibers reinforced by interfacial complexation. *Compos. Sci. Technol.* **2020**, *194*, 108174. [CrossRef]
105. Krystyjan, M.; Khachatryan, G.; Grabacka, M.; Krzan, M.; Witczak, M.; Grzyb, J.; Woszczak, L. Physicochemical, Bacteriostatic, and Biological Properties of Starch/Chitosan Polymer Composites Modified by Graphene Oxide, Designed as New Bionanomaterials. *Polymers* **2021**, *13*, 2327. [CrossRef] [PubMed]
106. Shao, L.; Chang, X.; Zhang, Y.; Huang, Y.; Yao, Y.; Guo, Z. Graphene oxide cross-linked chitosan nanocomposite membrane. *Appl. Surf. Sci.* **2013**, *280*, 989–992. [CrossRef]
107. Lee, J.H.; Marroquin, J.; Rhee, K.Y.; Park, S.J.; Hui, D. Cryomilling application of graphene to improve material properties of graphene/chitosan nanocomposites. *Compos. Part B Eng.* **2013**, *45*, 682–687. [CrossRef]
108. Yang, X.; Tu, Y.; Li, L.; Shang, S.; Tao, X.M. Well-dispersed chitosan/graphene oxide nanocomposites. *ACS Appl. Mater. Interfaces* **2010**, *2*, 1707–1713. [CrossRef]
109. Delbecq, F. Supramolecular gels from lipopeptide gelators: Template improvement and strategies for the in-situ preparation of inorganic nanomaterials and for the dispersion of carbon nanomaterials. *Adv. Colloid Interface Sci.* **2014**, *209*, 98–108. [CrossRef]
110. Hejjaji, E.M.; Smith, A.M.; Morris, G.A. Designing chitosan-tripolyphosphate microparticles with desired size for specific pharmaceutical or forensic applications. *Int. J. Biol. Macromol.* **2017**, *95*, 564–573. [CrossRef]
111. Terzopoulou, Z.; Kyzas, G.Z.; Bikiaris, D.N. Recent advances in nanocomposite materials of graphene derivatives with polysaccharides. *Materials* **2015**, *8*, 652–683. [CrossRef]
112. Layek, R.K.; Samanta, S.; Nandi, A.K. Graphene sulphonic acid/chitosan nano biocomposites with tunable mechanical and conductivity properties. *Polymer* **2012**, *53*, 2265–2273. [CrossRef]
113. Han, D.; Yan, L. Supramolecular hydrogel of chitosan in the presence of graphene oxide nanosheets as 2D cross-linkers. *ACS Sustain. Chem. Eng.* **2014**, *2*, 296–300. [CrossRef]
114. Suri, A.; Khandegar, V.; Kaur, P.J. Ofloxacin exclusion using novel HRP immobilized chitosan cross-link with graphene-oxide nanocomposite. *Groundw. Sustain. Dev.* **2021**, *12*, 100515. [CrossRef]
115. Khan, Y.H.; Islam, A.; Sarwar, A.; Gull, N.; Khan, S.M.; Munawar, M.A.; Zia, S.; Sabir, A.; Shafiq, M.; Jamil, T. Novel green nano composites films fabricated by indigenously synthesized graphene oxide and chitosan. *Carbohydr. Polym.* **2016**, *146*, 131–138. [CrossRef] [PubMed]
116. Tan, C.P.; Zawawi, R.M.; ZA, N.H. Effect of sonication time and heat treatment on the structural and physical properties of chitosan/graphene oxide nanocomposite films. *Food Packag. Shelf Life* **2021**, *28*, 100663.
117. Cobos, M.; González, B.; Fernández, M.J.; Fernández, M.D. Study on the effect of graphene and glycerol plasticizer on the properties of chitosan-graphene nanocomposites via in situ green chemical reduction of graphene oxide. *Int. J. Biol. Macromol.* **2018**, *114*, 599–613. [CrossRef]
118. Kumar, S.; Wani, M.Y.; Koh, J.; Gil, J.M.; Sobral, A.J. Carbon dioxide adsorption and cycloaddition reaction of epoxides using chitosan–graphene oxide nanocomposite as a catalyst. *J. Environ. Sci.* **2018**, *69*, 77–84. [CrossRef]
119. Huang, J.; Jacobsen, J.; Larsen, S.W.; Genina, N.; Van de Weert, M.; Müllertz, A.; Nielsen, H.M.; Mu, H. Graphene oxide as a functional excipient in buccal films for delivery of clotrimazole: Effect of molecular interactions on drug release and antifungal activity in vitro. *Int. J. Pharm.* **2020**, *589*, 119811. [CrossRef]
120. Zhang, Q.; Cheng, W.; Wu, D.; Yang, Y.; Feng, X.; Gao, C.; Meng, L.; Shen, X.; Zhang, Y.; Tang, X. An electrochemical method for determination of amaranth in drinks using functionalized graphene oxide/chitosan/ionic liquid nanocomposite supported nanoporous gold. *Food Chem.* **2022**, *367*, 130727. [CrossRef]
121. da Silva, S.B.; Batista, G.L.; Santin, C.K. Chitosan for Sensors and Electrochemical Applications. In *Chitin and Chitosan*; Lambertus, A.M., van den, B., Boeriu, C.G., Eds.; Wiley: Hoboken, NJ, USA, 2019; Chapter 18; pp. 461–476.
122. Vinodh, R.; Sasikumar, Y.; Kim, H.J.; Atchudan, R.; Yi, M. Chitin and Chitosan Based Biopolymer Derived Electrode Materials for Supercapacitor Applications: A Critical Review. *J. Ind. Eng. Chem.* **2021**, in press. [CrossRef]
123. Wang, C.; Esker, A.R. Nanocrystalline chitin thin films. *Carbohydr. Polym.* **2014**, *102*, 151–158. [CrossRef] [PubMed]
124. Lizundia, E.; Nguyen, T.D.; Winnick, R.J.; MacLachlan, M.J. Biomimetic photonic materials derived from chitin and chitosan. *J. Mater. Chem. C* **2021**, *9*, 796–817. [CrossRef]
125. Kim, S.J.; Hong, B.M.; Park, W.H. The effects of chitin/chitosan nanowhiskers on the thermal, mechanical and dye adsorption properties of electrospun PVA nanofibrous membranes. *Cellulose* **2020**, *27*, 5771–5783. [CrossRef]
126. Saleh, T.A.; Parthasarathy, P.; Irfan, M. Advanced functional polymer nanocomposites and their use in water ultra-purification. *Trends Environ. Anal. Chem.* **2019**, *24*, e00067. [CrossRef]
127. Singh, R.P.; Singh, P.; Singh, K.R. Introduction to Composite Materials: Nanocomposites and Their Potential Applications. In *Composite Materials*; CRC Press: Boca Raton, FL, USA, 2021; pp. 1–28.
128. Pagliaro, M.; Ciriminna, R.; Yusuf, M.; Eskandarinezhad, S.; Wani, I.A.; Ghahremani, M.; Nezhad, Z.R. Application of nanocellulose composites in the environmental engineering as a catalyst, flocculants, and energy storages: A review. *J. Compos. Compd.* **2021**, *3*, 114–128.
129. Omran, A.A.B.; Mohammed, A.A.; Sapuan, S.M.; Ilyas, R.A.; Asyraf, M.R.M.; Rahimian Koloor, S.S.; Petrů, M. Micro- and nanocellulose in polymer composite materials: A review. *Polymers* **2021**, *13*, 231. [CrossRef] [PubMed]

130. Jafarzadeh, S.; Nafchi, A.M.; Salehabadi, A.; Oladzad-Abbasabadi, N.; Jafari, S.M. Application of bio-nanocomposite films and edible coatings for extending the shelf life of fresh fruits and vegetables. *Adv. Colloid Interface Sci.* **2021**, *291*, 102405. [CrossRef] [PubMed]
131. Jung, S.; Cui, Y.; Barnes, M.; Satam, C.; Zhang, S.; Chowdhury, R.A.; Adumbumkulath, A.; Sahin, O.; Miller, C.; Sajadi, S.M.; et al. Multifunctional Bio-Nanocomposite Coatings for Perishable Fruits. *Adv. Mater.* **2020**, *32*, 1908291. [CrossRef] [PubMed]
132. Nguyen, L.D.; Doan, T.C.D.; Huynh, T.M.; Nguyen, V.N.P.; Dinh, H.H.; Dang, D.M.T.; Dang, C.M. An electrochemical sensor based on polyvinyl alcohol/chitosan-thermally reduced graphene composite modified glassy carbon electrode for sensitive voltammetric detection of lead. *Sens. Actuators B Chem.* **2021**, *345*, 130443. [CrossRef]
133. Xie, P.; Yuan, W.; Liu, X.; Peng, Y.; Yin, Y.; Li, Y.; Wu, Z. Advanced carbon nanomaterials for state-of-the-art flexible supercapacitors. *Energy Storage Mater.* **2020**, *36*, 56–76. [CrossRef]
134. Li, W.; Song, B.; Zhang, S.; Zhang, F.; Liu, C.; Zhang, N.; Yao, H.; Shi, Y. Using 3-Isocyanatopropyltrimethoxysilane to decorate graphene oxide with nano-titanium dioxide for enhancing the anti-corrosion properties of epoxy coating. *Polymers* **2020**, *12*, 837. [CrossRef]
135. Veeralingam, S.; Badhulika, S. 2D-$SnSe_2$ nanoflakes on paper with 1D-NiO gate insulator based MISFET as multifunctional NIR photo switch and flexible temperature sensor. *Mater. Sci. Semicond. Process.* **2020**, *105*, 104738. [CrossRef]
136. Park, S.G.; Lee, K.H.; Lee, J.H.; Bang, G.; Kim, J.; Park, H.J.; Oh, M.S.; Lee, S.; Kim, Y.H.; Kim, Y.M.; et al. Improved polaronic transport under a strong Mott–Hubbard interaction in Cu-substituted NiO. *Inorg. Chem. Front.* **2020**, *7*, 853–858. [CrossRef]
137. Nasrollahzadeh, M.; Sajjadi, M.; Iravani, S.; Varma, R.S. Starch, cellulose, pectin, gum, alginate, chitin and chitosan derived (nano) materials for sustainable water treatment: A review. *Carbohydr. Polym.* **2020**, *251*, 116986. [CrossRef] [PubMed]
138. Zhai, X.; Zhang, C.; Zhao, G.; Stoll, S.; Ren, F.; Leng, X. Antioxidant capacities of the selenium nanoparticles stabilized by chitosan. *J. Nanobiotechnology* **2017**, *15*, 1–12. [CrossRef] [PubMed]
139. Magerusan, L.; Pogacean, F.; Coros, M.; Socaci, C.; Pruneanu, S.; Leostean, C.; Pana, I.O. Green methodology for the preparation of chitosan/graphene nanomaterial through electrochemical exfoliation and its applicability in Sunset Yellow detection. *Electrochim. Acta* **2018**, *283*, 578–589. [CrossRef]
140. Kamran, U.; Park, S.J. Tuning ratios of KOH and NaOH on acetic acid-mediated chitosan-based porous carbons for improving their textural features and $CO_2$ uptakes. *J. CO2 Util.* **2020**, *40*, 101212. [CrossRef]
141. Al-Mokaram, A.; Amir, M.A.; Yahya, R.; Abdi, M.M.; Mahmud, H.N.M.E. The development of non-enzymatic glucose biosensors based on electrochemically prepared polypyrrole–chitosan–titanium dioxide nanocomposite films. *Nanomaterials* **2017**, *7*, 129. [CrossRef]
142. Gupta, R.; Goddard, N.J. A study of diffraction-based chitosan leaky waveguide (LW) biosensors. *Analyst* **2021**, *146*, 4964–4971. [CrossRef] [PubMed]
143. Wei, P.; Zhu, Z.; Song, R.; Li, Z.; Chen, C. An ion-imprinted sensor based on chitosan-graphene oxide composite polymer modified glassy carbon electrode for environmental sensing application. *Electrochim. Acta* **2019**, *317*, 93–101. [CrossRef]
144. Fartas, F.M.; Abdullah, J.; Yusof, N.A.; Sulaiman, Y.; Saiman, M.I. Biosensor based on tyrosinase immobilized on graphene-decorated gold nanoparticle/chitosan for phenolic detection in aqueous. *Sensors* **2017**, *17*, 1132. [CrossRef]
145. Casteleijn, M.G.; Richardson, D.; Parkkila, P.; Granqvist, N.; Urtti, A.; Viitala, T. Spin coated chitin films for biosensors and its analysis are dependent on chitin-surface interactions. *Colloids Surf. A Physicochem. Eng. Asp.* **2018**, *539*, 261–272. [CrossRef]
146. Saleviter, S.; Fen, Y.W.; Omar, N.A.S.; Zainudin, A.A.; Daniyal, W.M.E.M.M. Optical and structural characterization of immobilized 4-(2-pyridylazo) resorcinol in chitosan-graphene oxide composite thin film and its potential for $Co^{2+}$ sensing using surface plasmon resonance technique. *Results Phys.* **2018**, *11*, 118–122. [CrossRef]
147. Ali, F.I.; Mahmoud, S.T.; Awwad, F.; Greish, Y.E.; Abu-Hani, A.F. Low power consumption and fast response $H_2S$ gas sensor based on a chitosan-CuO hybrid nanocomposite thin film. *Carbohydr. Polym.* **2020**, *236*, 116064. [CrossRef]
148. Borgohain, R.; Boruah, P.K.; Baruah, S. Heavy-metal ion sensor using chitosan capped ZnS quantum dots. *Sens. Actuators B Chem.* **2016**, *226*, 534–539. [CrossRef]
149. Conder, J.; Vaulot, C.; Marino, C.; Villevieille, C.; Ghimbeu, C.M. Chitin and chitosan—Structurally related precursors of dissimilar hard carbons for Na-ion battery. *ACS Appl. Energy Mater.* **2019**, *2*, 4841–4852. [CrossRef]
150. Chai, L.; Qu, Q.; Zhang, L.; Shen, M.; Zhang, L.; Zheng, H. Chitosan, a new and environmental benign electrode binder for use with graphite anode in lithium-ion batteries. *Electrochim. Acta* **2013**, *105*, 378–383. [CrossRef]
151. Ma, L.; Zhou, X.; Xu, L.; Xu, X.; Zhang, L.; Chen, W. Chitosan-assisted fabrication of ultrathin MoS2/graphene heterostructures for Li-ion battery with excellent electrochemical performance. *Electrochim. Acta* **2015**, *167*, 39–47. [CrossRef]
152. Chen, D.; Zhan, W.; Fu, X.; Zhu, M.; Lan, J.; Sui, G.; Yang, X. High-conductivity 1T-MoS 2 catalysts anchored on a carbon fiber cloth for high-performance lithium–sulfur batteries. *Mater. Chem. Front.* **2021**, *5*, 6941–6950. [CrossRef]
153. Kim, S.; Cho, M.; Lee, Y. Multifunctional chitosan–RGO network binder for enhancing the cycle stability of Li–S batteries. *Adv. Funct. Mater.* **2020**, *30*, 1907680. [CrossRef]
154. Jin, H.; Zhu, M.; Liu, J.; Gan, L.; Gong, Z.; Long, M. Alkaline chitosan solution as etching phase to design Si@ SiO2@ N-Carbon anode for Lithium-ion battery. *Appl. Surf. Sci.* **2021**, *541*, 148436. [CrossRef]
155. Wang, D.; Du, G.; Han, D.; Su, Q.; Ding, S.; Zhang, M.; Zhao, W.; Xu, B. Porous flexible nitrogen-rich carbon membranes derived from chitosan as free-standing anodes for potassium-ion and sodium-ion batteries. *Carbon* **2021**, *181*, 1–8. [CrossRef]

156. Sim, G.S.; Santhoshkumar, P.; Park, J.W.; Ho, C.W.; Shaji, N.; Kim, H.K.; Nanthagopal, M.; Lee, C.W. Chitosan-derived nitrogen-doped carbon on Li2ZnTi3O8/TiO2 composite as an anode material for lithium-ion batteries. *Ceram. Int.* **2021**, in press. [CrossRef]
157. Liu, C.; Li, R.; Liu, W.; Shen, G.; Chen, D. Chitosan-Assisted Fabrication of a Network C@ V2O5 Cathode for High-Performance Zn-Ion Batteries. *ACS Appl. Mater. Interfaces* **2021**, *13*, 37194–37200. [CrossRef]
158. Yu, L.; Liu, J.; He, S.; Huang, C.; Gong, Z.; Gan, L.; Long, M. N-doped rGO/C@ Si composites using sustainable chitosan as the carbon source for lithium-ion batteries. *Appl. Surf. Sci.* **2020**, *501*, 144136. [CrossRef]
159. Yang, Z.; Jia, D.; Wu, Y.; Song, D.; Sun, X.; Wang, C.; Yang, L.; Zhang, Y.; Gao, J.; Ohsaka, T.; et al. Novel Lithium-Chalcogenide Batteries Combining S, Se and C Characteristics Supported by Chitosan-Derived Carbon Intertwined with CNTs. *Chem. Eng. J.* **2021**, *427*, 131790. [CrossRef]
160. Nasirinezhad, M.; Ghaffarian, S.R.; Tohidian, M. Eco-friendly polyelectrolyte nanocomposite membranes based on chitosan and sulfonated chitin nanowhiskers for fuel cell applications. *Iran. Polym. J.* **2021**, *30*, 355–367. [CrossRef]
161. Li, S.W.; He, H.; Zeng, R.J.; Sheng, G.P. Chitin degradation and electricity generation by Aeromonas hydrophila in microbial fuel cells. *Chemosphere* **2017**, *168*, 293–299. [CrossRef]
162. Yang, W.; Wang, X.; Rossi, R.; Logan, B.E. Low-cost Fe–N–C catalyst derived from Fe (III)-chitosan hydrogel to enhance power production in microbial fuel cells. *Chem. Eng. J.* **2020**, *380*, 122522. [CrossRef]
163. Abu-Saied, M.A.; Soliman, E.A.; Al Desouki, E.A. Development of Proton Exchange Membranes Based on Chitosan Blended with Poly (2-Acrylamido-2-Methylpropane Sulfonic Acid) for Fuel Cells applications. *Mater. Today Commun.* **2020**, *25*, 101536. [CrossRef]
164. ul Haque, S.; Nasar, A.; Rahman, M.M. Applications of chitosan (CHI)-reduced graphene oxide (rGO)-polyaniline (PAni) conducting composite electrode for energy generation in glucose biofuel cell. *Sci. Rep.* **2020**, *10*, 1–12. [CrossRef] [PubMed]
165. Gorgieva, S.; Osmić, A.; Hribernik, S.; Božič, M.; Svete, J.; Hacker, V.; Wolf, S.; Genorio, B. Efficient Chitosan/Nitrogen-Doped Reduced Graphene Oxide Composite Membranes for Direct Alkaline Ethanol Fuel Cells. *Int. J. Mol. Sci.* **2021**, *22*, 1740. [CrossRef] [PubMed]
166. Yousefi, V.; Mohebbi-Kalhori, D.; Samimi, A. Start-up investigation of the self-assembled chitosan/montmorillonite nanocomposite over the ceramic support as a low-cost membrane for microbial fuel cell application. *Int. J. Hydrog. Energy* **2020**, *45*, 4804–4820. [CrossRef]
167. Zhang, G.; Li, L.; Chen, M.; Yang, F. Chitosan cross-linked poly (aminoanthraquinone)/Prussian blue ternary nitrogen precursor-derived Fe–N–C oxygen reduction catalysts for microbial fuel cells and zinc–air batteries. *J. Mater. Chem. A* **2020**, *8*, 9256–9267. [CrossRef]
168. Vijayalekshmi, V.; Khastgir, D. Eco-friendly methanesulfonic acid and sodium salt of dodecylbenzene sulfonic acid doped cross-linked chitosan based green polymer electrolyte membranes for fuel cell applications. *J. Membr. Sci.* **2017**, *523*, 45–59. [CrossRef]
169. Kaker, B.; Hribernik, S.; Mohan, T.; Kargl, R.; Stana Kleinschek, K.; Pavlica, E.; Kreta, A.; Bratina, G.; Lue, S.J.; Božič, M. Novel Chitosan–Mg $(OH)_2$-Based Nanocomposite Membranes for Direct Alkaline Ethanol Fuel Cells. *ACS Sustain. Chem. Eng.* **2019**, *7*, 19356–19368. [CrossRef]
170. Tohidian, M.; Ghaffarian, S.R. Polyelectrolyte nanocomposite membranes based on chitosan and surface modified multi-walled carbon nanotubes for use in fuel cell applications. *J. Macromol. Sci.* **2021**, *Part A*, 1–14.
171. Zhao, S.; Yang, Y.; Zhong, F.; Niu, W.; Liu, Y.; Zheng, G.; Liu, H.; Wang, J.; Xiao, Z. Fabrication of composite polymer electrolyte membrane using acidic metal-organic frameworks-functionalized halloysite nanotubes modified chitosan. *Polymer* **2021**, *226*, 123800. [CrossRef]
172. Roy, B.K.; Tahmid, I.; Rashid, T.U. Chitosan-Based Materials for Supercapacitor Application—A Review. *J. Mater. Chem. A* **2021**, *9*, 17592–17642. [CrossRef]
173. Cheng, J.; Xu, Q.; Wang, X.; Li, Z.; Wu, F.; Shao, J.; Xie, H. Ultrahigh-surface-area nitrogen-doped hierarchically porous carbon materials derived from chitosan and betaine hydrochloride sustainable precursors for high-performance supercapacitors. *Sustain. Energy Fuels* **2019**, *3*, 1215–1224. [CrossRef]
174. Suneetha, R.B.; Selvi, P.; Vedhi, C. Synthesis, structural and electrochemical characterization of Zn doped iron oxide/grapheneoxide/chitosan nanocomposite for supercapacitor application. *Vacuum* **2019**, *164*, 396–404. [CrossRef]
175. Yuan, M.; Zhang, Y.; Niu, B.; Jiang, F.; Yang, X.; Li, M. Chitosan-derived hybrid porous carbon with the novel tangerine pith-like surface as supercapacitor electrode. *J. Mater. Sci.* **2019**, *54*, 14456–14468. [CrossRef]
176. Chen, K.; Weng, S.; Lu, J.; Gu, J.; Chen, G.; Hu, O.; Jiang, X.; Hou, L. Facile synthesis of chitosan derived heteroatoms-doped hierarchical porous carbon for supercapacitors. *Microporous Mesoporous Mater.* **2021**, *320*, 111106. [CrossRef]
177. Lin, C.H.; Wang, P.H.; Lee, W.N.; Li, W.C.; Wen, T.C. Chitosan with various degrees of carboxylation as hydrogel electrolyte for pseudo solid-state supercapacitors. *J. Power Sources* **2021**, *494*, 229736. [CrossRef]
178. Zhang, K.; Xu, R.; Ge, W.; Qi, M.; Zhang, G.; Xu, Q.H.; Huang, F.; Cao, Y.; Wang, X. Electrostatically self-assembled chitosan derivatives working as efficient cathode interlayers for organic solar cells. *Nano Energy* **2017**, *34*, 164–171. [CrossRef]
179. Ababneh, H.; Hameed, B.H. Chitosan-derived hydrothermally carbonized materials and its applications: A review of recent literature. *Int. J. Biol. Macromol.* **2021**, *186*, 314–327. [CrossRef]

180. Praveen, E.; Peter, I.J.; Kumar, A.M.; Ramachandran, K.; Jayakumar, K. Boosting of power conversion efficiency of 2D ZnO nanostructures-based DSSC by the Lorentz force with chitosan polymer electrolyte. *J. Inorg. Organomet. Polym. Mater.* **2020**, *30*, 4927–4943. [CrossRef]
181. Rahman, N.A.; Hanifah, S.A.; Mobarak, N.N.; Ahmad, A.; Ludin, N.A.; Bella, F.; Su'ait, M.S. Chitosan as a paradigm for biopolymer electrolytes in solid-state dye-sensitised solar cells. *Polymer* **2021**, *230*, 124092. [CrossRef]
182. Pottathara, Y.B.; Reddy, H.; Tiyyagura, Z.A.; Thomas, S. Chitin and Chitosan Composites for Wearable Electronics and Energy Storage Devices. In *Handbook of Chitin and Chitosan: Volume 3: Chitin-and Chitosan-Based Polymer Materials for Various Applications*; Elsevier: Amsterdam, The Netherlands, 2020; Volume 73, p. 71.
183. Midya, L.; Chettri, A.; Pal, S. Development of a novel nanocomposite using polypyrrole grafted chitosan-decorated CDs with improved photocatalytic activity under solar light illumination. *ACS Sustain. Chem. Eng.* **2019**, *7*, 9416–9421. [CrossRef]
184. Zulkifli, A.M.; Said, N.I.A.M.; Bakr Aziz, S.; Dannoun, E.M.A.; Hisham, S.; Shah, S.; Abu Bakar, A.; Zainal, Z.H.; Tajuddin, H.A.; Mohammed Hadi, J.; et al. Characteristics of Dye-Sensitized Solar Cell Assembled from Modified Chitosan-Based Gel Polymer Electrolytes Incorporated with Potassium Iodide. *Molecules* **2020**, *25*, 4115. [CrossRef]
185. Yahya, W.Z.N.; Hong, P.Z.; Mohd Zain, W.Z.Z.W.; Mohamed, N.M. Tripropyl Chitosan Iodide-Based Gel Polymer Electrolyte as Quasi Solid-State Dye Sensitized Solar Cells. In *Materials Science Forum*; Trans Tech Publications Ltd.: Bäch SZ, Switzerland, 2020; Volume 997, pp. 69–76.
186. Abdulwahid, R.T.; Aziz, S.B.; Brza, M.A.; Kadir, M.F.Z.; Karim, W.O.; Hamsan, H.M.; Asnawi, A.S.; Abdullah, R.M.; Nofal, M.M.; Dannoun, E.M. Electrochemical performance of polymer blend electrolytes based on chitosan: Dextran: Impedance, dielectric properties, and energy storage study. *J. Mater. Sci. Mater. Electron.* **2021**, *32*, 1–17. [CrossRef]
187. Ali, A.; Alzamly, A.; Greish, Y.E.; Bakiro, M.; Nguyen, H.L.; Mahmoud, S.T. A Highly Sensitive and Flexible Metal–Organic Framework Polymer-Based $H_2S$ Gas Sensor. *ACS Omega* **2021**, *6*, 17690–17697. [CrossRef]
188. Nazari, F.; Ghoreishi, S.M.; Khoobi, A. Bio-based $Fe_3O_4$/chitosan nanocomposite sensor for response surface methodology and sensitive determination of gallic acid. *Int. J. Biol. Macromol.* **2020**, *160*, 456–469. [CrossRef]
189. Hussein, M.S.; Fekry, A.M. Effect of fumed silica/chitosan/poly (vinylpyrrolidone) composite coating on the electrochemical corrosion resistance of Ti–6Al–4V alloy in artificial saliva solution. *ACS Omega* **2019**, *4*, 73–78. [CrossRef]
190. Hwang, J.H.; Pathak, P.; Wang, X.; Rodriguez, K.L.; Park, J.; Cho, H.J.; Lee, W.H. A novel Fe-Chitosan-coated carbon electrode sensor for in situ As (III) detection in mining wastewater and soil leachate. *Sens. Actuators B: Chem.* **2019**, *294*, 89–97. [CrossRef]
191. Khalaf, N.; Ahamad, T.; Naushad, M.; Al-Hokbany, N.; Al-Saeedi, S.I.; Almotairi, S.; Alshehri, S.M. Chitosan polymer complex derived nanocomposite (AgNPs/NSC) for electrochemical non-enzymatic glucose sensor. *Int. J. Biol. Macromol.* **2020**, *146*, 763–772. [CrossRef] [PubMed]
192. Wu, J.; Li, H.; Lai, X.; Chen, Z.; Zeng, X. Conductive and superhydrophobic F-rGO@ CNTs/chitosan aerogel for piezoresistive pressure sensor. *Chem. Eng. J.* **2020**, *386*, 123998. [CrossRef]
193. Dai, H.; Feng, N.; Li, J.; Zhang, J.; Li, W. Chemiresistive humidity sensor based on chitosan/zinc oxide/single-walled carbon nanotube composite film. *Sens. Actuators B Chem.* **2019**, *283*, 786–792. [CrossRef]
194. Chen, T.W.; Chinnapaiyan, S.; Chen, S.M.; Ali, M.A.; Elshikh, M.S.; Mahmoud, A.H. Facile synthesis of copper ferrite nanoparticles with chitosan composite for high-performance electrochemical sensor. *Ultrason. Sonochem.* **2020**, *63*, 104902. [CrossRef]
195. Sadani, K.; Nag, P.; Mukherji, S. LSPR based optical fiber sensor with chitosan capped gold nanoparticles on BSA for trace detection of Hg (II) in water, soil and food samples. *Biosens. Bioelectron.* **2019**, *134*, 90–96. [CrossRef]
196. Qi, P.; Zhang, T.; Shao, J.; Yang, B.; Fei, T.; Wang, R. A QCM humidity sensor constructed by graphene quantum dots and chitosan composites. *Sens. Actuators A Phys.* **2019**, *287*, 93–101. [CrossRef]
197. Chen, S.; Qiu, L.; Cheng, H.M. Carbon-based fibers for advanced electrochemical energy storage devices. *Chem. Rev.* **2020**, *120*, 2811–2878. [CrossRef]
198. Jorge, F.E.; Pimenta, L.T.G.; Marques, M.D.F.V. Preparation and characterization of polyaniline nanocomposites with graphene oxide-zinc oxide hybrids in different morphologies. *Mater. Sci. Eng. B* **2021**, *263*, 114851. [CrossRef]
199. Aswathy, N.R.; Palai, A.K.; Ramadoss, A.; Mohanty, S.; Nayak, S.K. Fabrication of cellulose acetate-chitosan based flexible 3D scaffold-like porous membrane for supercapacitor applications with PVA gel electrolyte. *Cellulose* **2020**, *27*, 3871–3887. [CrossRef]
200. Zhong, S.; Kitta, M.; Xu, Q. Hierarchically Porous Carbons Derived from Metal–Organic Framework/Chitosan Composites for High-Performance Supercapacitors. *Chem. Asian J.* **2019**, *14*, 3583–3589. [CrossRef] [PubMed]
201. Qian, L.; Fan, Y.; Song, H.; Zhou, X.; Xiong, Y. Poly (ionic liquid)/carboxymethyl chitosan complex-derived nitrogen and sulfur codoped porous carbon for high-performance supercapacitors. *Ionics* **2019**, *25*, 4915–4924. [CrossRef]
202. Choosang, J.; Khumngern, S.; Thavarungkul, P.; Kanatharana, P.; Numnuam, A. An ultrasensitive label-free electrochemical immunosensor based on 3D porous chitosan–graphene–ionic liquid–ferrocene nanocomposite cryogel decorated with gold nanoparticles for prostate-specific antigen. *Talanta* **2021**, *224*, 121787. [CrossRef]
203. Hosseini, M.G.; Shahryari, E.; Yardani Sefidi, P. Polyaniline grafted chitosan/GO-CNT/$Fe_3O_4$ nanocomposite as a superior electrode material for supercapacitor application. *J. Appl. Polym. Sci.* **2021**, e50976. [CrossRef]
204. Gawad, S.A.; Nasr, A.; Fekry, A.M.; Filippov, L.O. Electrochemical and hydrogen evolution behaviour of a novel nano-cobalt/nano-chitosan composite coating on a surgical 316L stainless steel alloy as an implant. *Int. J. Hydrog. Energy* **2021**, *46*, 18233–18241. [CrossRef]

205. Zhang, T.W.; Shen, B.; Yao, H.B.; Ma, T.; Lu, L.L.; Zhou, F.; Yu, S.H. Prawn shell derived chitin nanofiber membranes as advanced sustainable separators for Li/Na-ion batteries. *Nano Lett.* **2017**, *17*, 4894–4901. [CrossRef]
206. Kim, J.K.; Kim, D.H.; Joo, S.H.; Choi, B.; Cha, A.; Kim, K.M.; Kwon, T.H.; Kwak, S.K.; Kang, S.J.; Jin, J. Hierarchical chitin fibers with aligned nanofibrillar architectures: A nonwoven-mat separator for lithium metal batteries. *ACS Nano* **2017**, *11*, 6114–6121. [CrossRef] [PubMed]
207. Divya, K.; Rana, D.; Rameesha, L.; Sri Abirami Saraswathi, M.S.; Nagendran, A. Highly selective custom-made chitosan based membranes with reduced fuel permeability for direct methanol fuel cells. *J. Appl. Polym. Sci.* **2021**, *138*, 51366. [CrossRef]
208. Shen, S.; Jia, T.; Jia, J.; Wang, N.; Song, D.; Zhao, J.; Jin, J.; Che, Q. Constructing anhydrous proton exchange membranes through alternate depositing graphene oxide and chitosan on sulfonated poly (vinylidenefluoride) or sulfonated poly (vinylidene fluoride-co-hexafluoropropylene) membranes. *Eur. Polym. J.* **2021**, *142*, 110160. [CrossRef]
209. Chadha, N.; Saini, P. Post synthesis foaming of graphene-oxide/chitosan aerogel for efficient microwave absorbers via regulation of multiple reflections. *Mater. Res. Bull.* **2021**, *143*, 111458. [CrossRef]
210. Youssef, A.M.; Hasanin, M.S.; Abd El-Aziz, M.E.; Turky, G.M. Conducting chitosan/hydroxylethyl cellulose/polyaniline bionanocomposites hydrogel based on graphene oxide doped with Ag-NPs. *Int. J. Biol. Macromol.* **2021**, *167*, 1435–1444. [CrossRef] [PubMed]
211. Aziz, S.B.; Nofal, M.M.; Abdulwahid, R.T.; Kadir, M.F.Z.; Hadi, J.M.; Hussien, M.M.; Kareem, W.O.; Dannoun, E.M.; Saeed, S.R. Impedance, FTIR and Transport Properties of Plasticized Proton Conducting Biopolymer Electrolyte Based on Chitosan for Electrochemical Device Application. *Results Phys.* **2021**, *29*, 104770. [CrossRef]